Cloud Removal Advances: A Comprehensive Review and Analysis for Optical Remote Sensing Images

Jin Ning¹⁰, Lianbin Xie¹⁰, Jie Yin, and Yiguang Liu¹⁰

Abstract—Cloud cover significantly decreases the quality of optical remote sensing (ORS) images, adversely impacting its effectiveness in geographic monitoring, disaster prevention, and advanced visual applications. This phenomenon has made cloud removal a critical preprocessing step in ORS image processing. This article comprehensively reviews cloud removal techniques and classifies them based on the type of auxiliary data used: single-image, multimodal, and multitemporal. The discussed methods include physical modeling, deep learning, multispectral analysis, and synthetic aperture radar (SAR) fusion strategies. This article analyzes the core concepts and fundamental processes of these techniques and addresses the challenges encountered in actual scenarios. The article also includes future research directions. Moreover, the article outlines the benchmark datasets and evaluation metrics commonly used in cloud removal, thereby establishing a standardized reference for algorithm development and performance evaluation. A thorough comparative analysis was performed to assess their performance variations using visualization outcomes from the most recent and representative methodologies.

Index Terms—Cloud removal, multimodal, multitemporal, optical remote sensing (ORS), single-image.

I. INTRODUCTION

PTICAL remote sensing (ORS) images are a vital Earth observation data source that can capture a wealth of information from the Earth's surface. The data can contribute significantly to diverse fields, including environmental monitoring, resource investigation, and disaster assessment [1]. However, ORS images are frequently impeded by cloud cover, which results in the distortion or absence of surface information. Consequently, the use of cloud removal techniques to retrieve surface information holds substantial theoretical significance and practical necessity [2]. ORS image cloud removal aims to mitigate or eliminate cloud influence, thereby revealing more accurate and complete surface details [3]. Nevertheless, the extensive coverage, strong occlusion, uneven distribution, and high

Received 1 April 2025; revised 13 May 2025 and 29 May 2025; accepted 15 June 2025. Date of publication 18 June 2025; date of current version 7 July 2025. This work was supported in part by the National Key Research and Development Program of China under Grant 2023YFF0615800, and in part by the Sichuan Province under Grant 2024ZHCG0169 and Grant 2023YFG0334. (Corresponding author: Yiguang Liu.)

Jin Ning, Lianbin Xie, and Jie Yin are with the College of Computer Science and Cyber Security (Pilot Software College), Chengdu University of Technology, Chengdu 610059, China (e-mail: ningjin@cdut.edu.cn; xielian-bin@stu.cdut.edu.cn; yinjie13@stu.cdut.edu.cn).

Yiguang Liu is with the College of Computer Science, Sichuan University, Chengdu 610065, China (e-mail: liuyg@scu.edu.cn).

Digital Object Identifier 10.1109/JSTARS.2025.3580718

similarity to certain ground objects of clouds pose multifaceted challenges for cloud removal techniques: (1) Reconstruction of damaged details, (2) recovery of missing information, (3) generalization performance of methods, and (4) data pairing and registration.

Constrained by the limited acquisition capabilities of early remote sensing data, some single-image cloud removal methods were initially proposed, drawing on the techniques of natural image dehazing. These methods leverage the OSR image alone, eschewing additional auxiliary data. It employs sophisticated image processing techniques, including spatial filtering, contrast enhancement, and image restoration [4], [5], [6]. More complex algorithms are also employed, such as prior knowledge and deep learning [7]. This method excels in scenarios with light cloud cover or clouds that are evenly distributed but performs poorly when faced with thick or irregularly distributed cloud cover [8]. To better capture and restore detailed ground information underneath thick clouds, several multimodal cloud removal methods have been developed [9], [10]. For instance, combining high-resolution, multispectral remote sensing data can more comprehensively capture the ground information [11]. Fusing SAR [12] data takes advantage of its cloud-penetrating capabilities to improve the recovery of detailed texture features [13]. Multimodal cloud removal is effective for both thin and thick clouds, particularly adept at managing complex cloud coverage scenarios [14], [15]. However, its implementation is more intricate and may introduce additional noise. As advancements in image processing and remote sensing have accelerated, several multitemporal cloud removal methods that utilize multitemporal images as auxiliary data have been proposed to more accurately remove thick clouds [16], [17]. By fusing images from the same location during distinct temporal intervals, it can discern the dynamic changes in clouds and the stable features of the ground [18], [19]. For example, when an image at a specific time is obscured by clouds, clear images from other times can be utilized to assist in restoration. This method excels in areas with extensive or thick cloud coverage but faces challenges with positional alignment and is not suitable for areas with significant ground feature changes [20]. The illustrative example images of single-image, multimodal, and multitemporal methods are shown in Fig. 1.

An exhaustive search was conducted for ORS image cloud removal within various academic literature databases, followed by a detailed analysis and organization of the findings to illustrate the research trends across the three methods. The number of documents spanning a nearly decade-long period from 2015

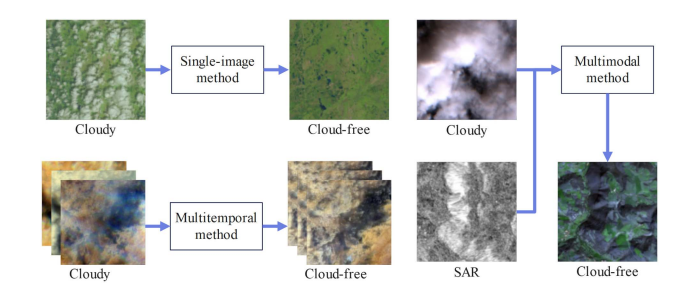


Fig. 1. Illustration of three types of ORS image cloud removal methods.

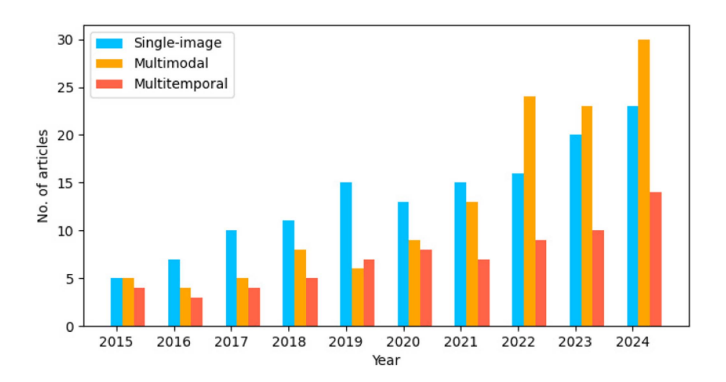


Fig. 2. Development trends of three types of ORS image cloud removal methods from 2015 to 2024.

to 2024 was tallied for each category, and these statistics were depicted as a histogram in Fig. 2. Multimodal methods have garnered growing interest over time, and this surge in attention can be attributed to the ability to furnish richer information, which enables higher precision and robustness. The single-image approaches have reached a plateau following an upward trend in advancement. This trend shows that these approaches continue to be effective in specific scenarios. Furthermore, although multitemporal methods offer distinctive advantages in addressing thick cloud issues, their complex data processing requirements have resulted in substantial potential for growth. In recent years, despite the thriving advancements in cloud removal techniques for ORS images, comprehensive review articles on the subject have been scarce. Xiong et al. [21] reviewed cloud removal in ORS images utilizing SAR fusion, yet their focus was primarily on GAN-based methods. Lee et al. [22] offered a more holistic overview of ORS image dehazing, encompassing remotely piloted aerial vehicle-based ORS image dehazing as well. Distinguished from these studies, this article initiates an exhaustive exploration of high-caliber research papers on ORS image cloud removal spanning the last decade, with particular emphasis on the most recent three years. By meticulously examining and analyzing these works, the approaches were categorized into three categories: single-image, multimodal, and multitemporal. Then, the foundational concepts, evolutionary trajectories, applicable contexts, and prospective avenues of these methods were outlined. The review encompasses the research status and the strengths and weaknesses of the subtechnologies within each category. Special emphasis is placed on key technologies such as physical modeling, deep learning, multispectral analysis, and SAR fusion. Finally, through comparative experimental analysis, further discussions were made on the current challenges and research analysis of each method. The main contributions of this article are as follows:

- This article meticulously categorizes the existing methods into three categories: single-image, multimodal, and multitemporal, elucidating the foundational concepts and underlying principles of each approach. By summarizing the current challenges and future outlook for these three approaches, the article contributes to a systematic understanding of ORS image cloud removal.
- 2) This review delves into key technologies including physical modeling, deep learning, multispectral analysis, and SAR fusion, highlighting the advantages and constraints inherent to each. Furthermore, it discusses the emerging trends of cross-integration among these technologies, offering a theoretical foundation for the development of hybrid and sophisticated cloud removal models.
- 3) Through quantitative and qualitative comparative experiments on representative datasets, a visual cloud removal effect analysis was conducted for the three types of methods. The article presents and discusses the current state of cloud removal technology, the challenges encountered, and the trends in research, thereby providing researchers with more profound theoretical and practical insights.

The rest of this article is organized as follows. Section II systematically reviews three categories of cloud removal methods: single-image based, multimodal-based, and multitemporal-based. Section III presents the commonly used datasets and evaluation metrics, provides experimental comparisons of representative methods, and discusses potential future directions. Finally, Section IV concludes this article.

II. CLOUD REMOVAL ADVANCES IN ORS IMAGES

This section provides a comprehensive review of cloud removal methods, focusing on three distinct categories: single-image, multimodal-based, and multitemporal-based. Single-image methods encompass statistical and physical model-based techniques, and deep learning-based methods. Multimodal-based approaches cover multispectral-based methods and SAR fusion-based techniques. Multitemporal-based methods include multitemporal nonblind and blind techniques. Each section concludes with a comprehensive summary of the current issues and future prospects pertinent to the respective methods.

A. Single-Image Cloud Removal

Single-image cloud removal leverages the available information from cloud-free regions to guide detail recovery in cloudy regions. This technique can suppress cloud components and enhance surface features, thereby improving image clarity. In addition, it is cost-effective and time-efficient, as it requires no additional data collection or processing. Based on the techniques used, existing methods can be broadly categorized into statistical and physical model-based methods, and deep learning-based methods [23], as shown in Table I.

TABLE I SUMMARY OF TYPICAL SINGLE-IMAGE METHODS

Class	Sub-Class	Authors and Year	Advantages	Limitations
		Zhang et al. [24],	Constructing a clear line of demarcation be-	Requirement for manual sample selection.
Statistical and Physical Model-	Physical	2002	tween cloud and surface pixels.	
	Model- based	He et al. [25], 2010	Avoiding dependence on training samples.	Darker than the real truth and often over- saturated.
		Hu et al. [26], 2015	Accurate processing in each frequency band by domain adaptation regression.	Unnatural color shifts exist.
		Wan et al. [27], 2016	Strong singularity capture ability.	Sensitivity to parameter selection.
		Zhao et al. [28], 2016	Ability to automatically recognize, remove and fill in cloudy areas.	Significant spliced seam marks.
		Xu et al. [29], 2019	Robust on Thin clouds.	Unsuitability for bright scenes.
		Shi et al. [30], 2021	Solving the color oversaturation problem.	Influenced by reference sample time interval.
		Zhang et al. [31],	Improved accuracy in distinguishing between	Noise in the declouded results.
based		2023	thin clouds and land surfaces.	
		Yang et al. [32], 2020	Outstanding detailed texture.	Ignoring geometric structure information.
	Deep	1 1221 2022		
	Learning- based	Wen et al. [33], 2022	Significant high-frequency detail on ground scenes.	Challenges in eliminating thick clouds.
		Zi et al. [34], 2023	Feeling wild with less loss of detail.	Computational expense of the model.
		Guo et al. [35], 2023	Ability to remove thin and small-scale thick clouds.	Poor performance on real clouds.
		Ning et al. [36], 2024	Well-characterized local details.	Difficulty in recovering features under thick clouds.
		Yan et al. [37], 2024	Better performance in ship detection tasks.	Poor performance when cloud coverage is too large.
		Jiang et al. [38], 2024	No cloud detection or cloud masking is required.	The visual performance of the cloud removal results is relatively poor.
		Li et al. [39], 2025	Chromatic aberration elimination.	Failure to recover extensive cloud coverage.
		Toizumi et al. [40], 2019	Thin cloud removal results in no artifacts.	Complex model training and requiring cloud masks.
	GAN- based	Li, et al. [41], 2020	Maximization of original background information preservation.	Declouded results with whitish color.
		Pan et al. [42], 2020	Well structure of the restored image.	Unrealistic feature textures or artifacts.
		Wen, et al. [43], 2021	Recovering images with more natural and realistic colors.	Poor generalization ability.
Deep Learning- based		Zhao et al. [44], 2021	Accurate learning of different ground information.	Artifacts in thick cloud output.
		Zhou et al. [45], 2022	Effectiveness for uniform thin clouds.	Inapplicability to non-uniform thin cloud situations.
		Liu et al. [46], 2022	Reconstructing partially thick cloud-obscured features.	Color mismatch of different land types in images.
		Ma et al. [47], 2023	Strong anti-interference performance when thick and thin clouds coexist.	Need for accurate cloud segmentation.
		Singh et al. [48], 2018	Generates images with fewer artifacts and improved realism.	Severe color shift.
	CycleGAN- based	Zi et al. [49], 2021	Excellent performance in thin cloud removal and color fidelity.	Inability to remove extensive cloud coverage.
		Mo, et al. [50], 2022	Specializing in dense haze.	Color distortion in the sky area.
		Jaisurya, et al. [51], 2023	Effective uniform thin and thick haze treatment.	Severe color disorder in handling bright objects.
		Ye et al. [52], 2024	Strong adaptive repair capability.	Difficulty in meeting physical consistency requirements in actual situations.

1) Statistical and Physical Model-Based Methods: Statistical and physical model-based methods posit that there are inherent statistical patterns or physical property differences between missing and valid data in a cloudy image, which can be used to efficiently separate cloud layer and repair damaged regions. Consequently, the spatial correlations and frequency differences between cloudy and cloud-free areas, as well as physical imaging models, can be employed to reconstruct clear regions.

Spatial-based methods [29], [53], [54] assume that the missing and valid data exhibit similar statistical characteristics or textural information, and this similarity helps estimate missing data to produce a visually consistent cloud-free image. Nonetheless, spatial-based methods are limited in removing only speckled clouds, and the semantic information restored under extensive cloud cover often deviates significantly from the original data.

Frequency-based methods [26], [27], [28], [55], [56] leverage the low-frequency attributes of thin clouds to design low-pass filters. These filters are employed to separate the thin cloud layer, which is subsequently utilized to suppress the target thin cloud. However, determining the optimal cutoff frequency for these frequency-based methods is typically challenging and can lead to the loss of original low-frequency information in cloud-free regions. Physical-based methods adhere to the principles of atmospheric imaging and are meticulously designed to account for atmospheric scattering and absorption effects. By accurately estimating and adjusting atmospheric parameters, these methods can effectively remove thin clouds. For instance, prior-based approaches estimate the transmission map t(x) and the global atmospheric light A based on prior assumptions to restore the cloud-free image J(x) within the atmospheric scattering

model defined by I(x) = J(x)t(x) + A(1-t(x)) [57]. Zhang et al. [24] proposed an atmospheric correction technique that treats all pixels equally. He et al. [25] introduced the dark channel prior (DCP) that proves effective for thin cloud removal tasks [30], [31]. However, inaccurate estimations of atmospheric parameters can significantly impact the cloud removal effect, potentially resulting in residual clouds or artifacts.

Statistical and physical model-based methods boast high theoretical clarity and are effective for processing uniform thin clouds. These approaches involve either identifying statistical patterns across various dimensions from cloudy images to cloud-free images or estimating model-related parameters. Nonetheless, under complex and variable meteorological conditions, the pattern assumptions may not be entirely satisfied, resulting in suboptimal cloud removal results.

2) Deep Learning-Based Methods: With the relentless progress in deep learning, single-image cloud removal based on it have gained broad prospects [58]. These methods construct deep neural networks to learn the complex relationships between cloudy and clear images, thereby removing clouds more accurately. Deep learning-based cloud removal methods can effectively eliminate cloud obstructions and enhance image quality, marking a breakthrough in cloud removal for single ORS images.

Convolutional neural network (CNN), leveraging its robust data fitting capabilities, is increasingly being utilized for cloud removal and have achieved impressive performance in eliminating thin clouds. CNN-based single-image cloud removal methods reconstruct clear images by learning the nonlinear mapping between cloudy and cloud-free images. To enhance visual quality, various techniques have been implemented for superior restoration effects. For instance, residual blocks [59] can alleviate the damage induced by additive noise, multiscale convolutions [32], [60] are adept at capturing fine-grained detail features, and attention mechanisms [33] direct the network to concentrate on key features. However, the fixed kernel size in CNNs restricts the engagement between the overall and detailed elements of the image, causing artifacts or residual clouds in the cloud removal outcomes.

Some methods [37], [61] leverage a U-shaped encoderdecoder structure to reconstruct cloud-free images, integrating features from encoding stages directly to their respective decoding stages through skip connections. Nevertheless, directly learning the mapping from cloudy to cloud-free images lacks interpretability. To address this challenge, some methods [34], [35], [36], [38] attempt to integrate CNNs with the frequency domain properties. The commonly used U-Net architecture as shown in Fig. 3. However, these U-Net-based methods struggle to effectively incorporate both low-level and high-level features, resulting in many detailed features being ignored. Furthermore, the end-to-end learning network demands a substantial collection of artificially synthesized paired images for training, resulting in suboptimal generalization capabilities of the model when applied to real-world scenarios. Adversarial learning has emerged as one of the most promising unsupervised methods for studying complex distributions in recent years. Generative

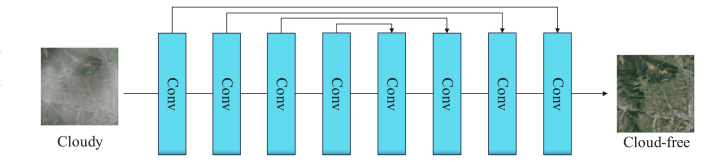


Fig. 3. U-Net architecture for single-image cloud removal methods is characterized by convolutional blocks with invariant feature sizes and residual connections [36].

adversarial network (GAN), typically consists of two components: a generator and a discriminator. Through adversarial training with the discriminator, the generator can learn cloudy features from unlabeled data, reducing the dependency on highquality annotated datasets [40], [41], [42], [43], [44], [45], [46], [47]. Despite the strong generalization performance of unidirectional GANs on real cloudy images, their cloud removal effect still needs to be improved due to the lack of cloud-free labels. Recently, CycleGAN [48], [49], [50], [51], [52] has been widely applied in image restoration. It endeavors to establish bidirectional mappings between different domains, utilizing cycle consistency loss and identity loss to preserve color compositions and textures effectively. The CycleGAN design principle constrains the transformation between two domains through cyclic consistency. However, the CycleGANbased methods have limitations in globally capturing the integrated data distribution [62], resulting in asymmetric domain knowledge from the source to the target and poor visualization when reconstructing texture details in cloud-covered

Deep learning-based single-image cloud removal exhibit robust feature extraction capabilities, allowing them to learn the mapping between cloudy and clear images. Despite these strengths, they also have limitations such as data dependency and computational consumption [63], [64]. In addition, within the constraint of single-image cloud removal, features completely obscured by thick clouds are difficult to be learned.

3) Current Issues and Future Prospects: Single-image cloud removal techniques are advantageous due to their minimal reliance on additional auxiliary data, which significantly reduces both the cost and complexity associated with data acquisition. They excel at removing thin clouds. Nonetheless, these techniques face challenges in eliminating dense clouds and cloud shadows, leading to the introduction of artifacts or color distortion. For complex cloud scenes, the accuracy and robustness of these methods are often found to be suboptimal [49].

As remote sensing and computer vision technologies continue to advance, single-image cloud removal techniques are poised to make significant strides and breakthroughs in the future. On the one hand, it is possible to better learn the differences between clouds and ground objects by developing more advanced neural network models, thereby removing clouds more accurately. On the other hand, the model's generalization ability can be enhanced by leveraging GAN-based unpaired learning mechanisms. In addition, a more comprehensive pipeline for processing ORS images can be established by integrating

Class	Sub-Class Authors and Year Advantages		Limitations			
		Czerkawski et al. [72], 2019	Good seasonal adaptability.	Reliance on high-quality masks.		
	Conventional Algorithms	Cheng et al. [73],	Well-defined outlines in cloud removal results.	Inapplicability to non-uniform cloud coverage.		
		Wang et al. [74], 2022	Computational efficiency.	Incomplete utilization of information from each spectral band.		
		Guo et al. [35], 2023	Good visual quality.	Poor generalization capability for cloud removal.		
		Arp et al. [75], 2024	Capable of restoring small ground textures.	Poor pixel-level recovery performance.		
Multispectral- based	-	Zhang et al. [77], 2024	Compatible with various satellite data.	Relies on the accuracy of cloud detection.		
-		Guo et al. [77], 2020	Performs well in vegetated scenarios.	Diminished effectiveness under high cloud cover.		
		Zi et al. [78], 2021	Good color fidelity.	Texture inconsistency in restoration results.		
	Deep Learning	Ghozatlou et al. [13], 2021	Capable of removing cloud shadows.	Performance is poor with substantial cloud coverage.		
		Li et al. [79], 2022	Performs well in vegetated scenarios.	Performance is suboptimal under thick cloud conditions.		
		Lyu et al. [4], 2023	Capable of removing cirrus clouds.	Inapplicability to moderate to heavy cloud cover scenarios.		
		Zhao et al. [80], 2024	Good generalization in thin cloud removal.	Poor cloud removal performance in complex scenes.		
		Gao et al. [81], 2020	Capable of eliminating imaging artifacts.	Scenario-specific pre-training requirements.		
	GAN	Li et al. [82], 2022	Cloud suppression in maritime scenarios.	Requirement for high-quality auxiliary annotations.		
		Zhou et al. [45], 2022	Consistency of cloud-free region texture with real areas.	Inability to generate spectral information for thick cloud-obscured features.		
		Hao et al. [83], 2023	Effective reduction of noise and redundant information.	Suboptimal restoration of fine textures in land- scapes.		
		Li et al. [84], 2023	Optimized visual output quality.	High parameter count of the model.		
SAR -		Wang et al. [85], 2025	Mitigated spot noise.	Spectral distortion.		
Fusion-		Chen et al. [68], 2022	Superior visual perception performance.	Degraded performance in complex texture scenarios.		
based	Non-GAN	Xu et al. [86], 2022	Mitigation speckle noise-induced performance degradation.	Compromised efficacy in high-cloud-cover scenarios.		
		Han et al. [70], 2023	Enhanced chromatic fidelity.	Dimensionality constraints in multi-channel image processing.		
		Wen et al. [87], 2023	Enhanced edge delineation capability.	Constrained recovery of textural minutiae under high-frequency components.		
		Duan et al. [88], 2024	Accelerated cloud removal throughput.	Suboptimal visual output quality under full- spectrum rendering.		
		Yu et al. [89], 2024	Enhanced cross-domain adaptability.	Blurry reconstruction results.		
		Zou et al. [90], 2024	Superior image fidelity compliance.	Poor visual effects in complex scenes.		

TABLE II
SUMMARY OF TYPICAL MULTIMODAL-BASED METHODS

multitask learning mechanisms with other cutting-edge computer vision technologies.

B. Multimodal-Based Cloud Removal

To tackle the challenges associated with thick cloud removal from single ORS image, researchers employ multimodal data as supplementary information to enhance the removal quality. These multimodal data are gathered from various sensors, each exhibiting unique imaging properties [65], [66], [67]. Multimodal-based approaches reconstruct thick cloud areas by integrating complementary information from different modality images, effectively overcoming the constraints inherent in single-modal data [68], [69], [70]. These approaches are capable of more accurately removing different types of clouds and adapting to various land cover types, demonstrating high adaptability and reliability. Depending on the varying types of auxiliary modal data, these approaches can generally be categorized into two major groups: multispectral-based methods and SAR fusion-based methods [71], as shown in Table II.

1) Multispectral-Based Methods: Different spectral bands exhibit varying sensitivities to cloud features, thus they can provide distinct information regarding both cloud and surface characteristics. Multispectral-based cloud removal leverages these abundant information from diverse spectral bands to identify and reconstruct the cloudy areas, significantly enhancing the quality in thin and semitransparent clouds [91], [92].

Multispectral-based cloud removal techniques primarily rely on spectral features, physical attributes, and statistical analysis to discern the spectral and textural signatures of clouds, as well as their spatial distribution. They utilize conventional algorithms including filtering, interpolation, and substitution to eliminate cloud cover [93], [94], [95], [96], [97]. The aforementioned methods demand a deep comprehension of ORS images and cloud characteristics, coupled with substantial experience in image processing. They are adept at accurately restoring the radiative properties while exerting a negligible influence on cloud-free areas. However, these methods require accurate estimation of physical parameters, which inherently increases the complexity of their application. In addition, they necessitate professional expertise, which limits their effectiveness in addressing complex scenarios, resulting in a relatively weak capacity for generalization [98].

With the continuous advancement of algorithms and hardware, deep learning shows broad application prospects in the field of multispectral cloud removal [99]. Through the training on extensive annotated datasets, deep learning techniques can automatically extract features of land objects and eliminate cloud obstructions [100], [101]. The frequently utilized deep learning framework as shown in Fig. 4. Hao et al. [83] and Guo et al. [77] leveraged channel attention mechanisms to capture significant information across different channels. Zhao et al. [80] integrated spatial attention, channel attention, and multiscale convolutional networks to bolster the capability of detecting thin

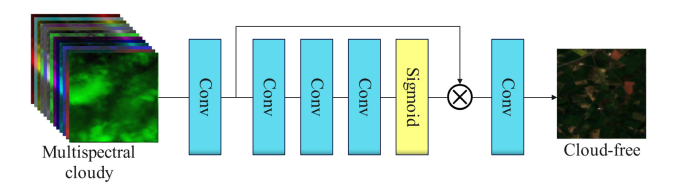


Fig. 4. Frequently utilized deep learning framework for multispectral-based cloud removal methods [80]. This framework combines cross-channel feature enhancement modules with sigmoid-activated residual pathways, enabling adaptive spectral feature recalibration.

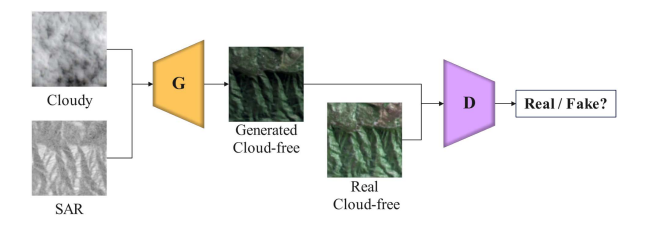


Fig. 5. Commonly used GAN framework for cloud removal based on SAR fusion [84]: G aims to generate cloud-free images, and D aims to determine the authenticity of the images generated by G.

cloud distributions. However, deep learning methods frequently depend on sizable labeled datasets and advanced hardware infrastructure. Moreover, these models tend to have limited interpretability and can introduce noise postcloud removal [102].

Multispectral cloud removal techniques capitalize on the inherent strengths of satellite ORS, boasting considerable advantages in the quality and precision of cloud removal. Nevertheless, the spectral bands are highly vulnerable to interference from dense cloud cover, which exacerbates the challenge of retrieving surface information.

2) SAR Fusion-Based Methods: SAR is a proactive microwave imaging approach that is capable of acquiring information about ground objects under a wide range of weather conditions [103]. This attribute enables it to penetrate through clouds to acquire surface information, providing a significant advantage for cloud removal [68]. SAR fusion-based methods utilize this unique advantage as auxiliary data to guide the texture recovery of ORS images.

In the early research stages, academics utilized GANs to fuse SAR with ORS images for cloud removal [104]. The commonly used GAN framework as shown in Fig. 5. Hao et al. [83] used GAN to selectively fuse information features to achieve cloud removal, and channel attention to improve feature recovery in cloud coverage areas. Li et al. [84] developed a Transformer-based GAN with a generator that adopts a hierarchical structure to capitalize on both the deep and shallow features of images, as well as the global-local geographical proximity. SAR fusion-based GANs can generate realistic images and show particular strength in handling complex cloudy structures and textures. Nonetheless, the training process of GAN models tends to be intricate, and the model's performance can be inconsistent, which may fall short of the desired cloud removal outcomes.

In recent years, several nonGAN approaches have demonstrated promising results in the effective removal of clouds. Xu et al. [86] proposed a fusion technique that integrates SAR

and ORS images globally and locally. Li et al. [69] introduced a structurally consistent fusion network that employs a channel attention mechanism to alleviate the pseudoartificial features induced by speckle noise. Zou et al. [90] utilized a conditional and denoising encoder to mitigate the impact of speckle noise. NonGAN models necessitate parameter adjustments specific to particular scenarios when processing ORS images that encompass diverse scenes and varying degrees of cloud coverage.

The integration of SAR images allows for more precise and comprehensive cloud removal [105]. However, effectively merging these distinct types of images continues to pose a significant challenge [106]. Current fusion methods often do not take full advantage of the complementary information between SAR and OSR images, which results in suboptimal cloud removal outcomes. In addition, SAR image quality plays a pivotal role in the efficacy of cloud removal techniques [107]. Noise or distortion present in the SAR images can be magnified during the cloud removal process, thereby compromising the final results.

3) Current Issues and Future Prospects: Multimodal-based methods have demonstrated significant promise due to their superior dependability, yet they encounter several challenges in real-world applications, including dataset inconsistency and lack of clear connections. The former issue arises from the necessity to manage extensive heterogeneous data, which complicates the design and implementation of algorithms. The latter issue is due to the absence of overt connections between disparate data sources, necessitating more sophisticated strategies to recognize and leverage complementary information. In the data fusion process, the disparities in information across different modalities can result in the loss of certain image details, thereby impacting the quality of the final declouded image. SAR fusion-based methods demand substantial effort during the stages of data registration and preprocessing, and the presence of speckle noise can introduce artifacts.

In the future, there is an urgent need to further explore more effective multimodal data fusion strategies to generate more accurate and comprehensive cloud-free images. This entails leveraging the complementary information between different modalities to enhance integration. For example, global-local fusion algorithms can improve the utilization of SAR data, conditional GANs can bolster SAR-assisted cloud removal efforts, adaptive weight allocation can focus on key obscured areas, and multiscale feature extraction can adapt to varying resolutions and complexities.

C. Multitemporal-Based Cloud Removal

Remote sensing systems with periodic revisits are capable of acquiring multitemporal images of the same location [97], thus providing an additional auxiliary dataset for ORS image cloud removal. Typically, data collected over the same location at various time intervals are termed as multitemporal images. Given that the distribution of clouds may evolve over time, the cloud cover conditions differ across these multitemporal images [108]. Multitemporal cloud removal techniques leverage the complementary information present within multitemporal

Class SubClass Authors and Year Advantages			Limitations	
Non-blind		Bertoluzza et al. [95], 2019	Recovers semi-transparent data missing information.	Performance degrades with older data collection dates.
	Similarity- based	Shen et al. [96], 2019	Capable of processing scenarios with notable land cover variations.	Insufficient accuracy in feature detail reconstruction.
		Zhou et al. [98], 2023	Operates across seasonal variations.	Poor reconstruction performance with similar atmospheric conditions at multiple time points.
		Lin et al. [108], 2022	Ability to adapt to inaccurate mask conditions.	Dependency of cloud removal result on mask quality.
	Model- Based	Xia et al. [109], 2022	Significant improvement in reconstruction accuracy of cloud-covered areas.	Requirement for at least one cloud-free phase across all time phases.
Technique		Zheng et al. [110], 2023	Reduction of color error in cloud removal results.	Poor performance in texture details.
		Li et al. [111], 2023	Capability to restore fine edges and texture information.	Poor performance on large-scale thick clouds.
		Ji et al. [112], 2020	Elimination of need for manual labeling.	Poor performance in pixel-level reconstruction results.
	Deep Learning	Zhang et al. [113], 2020	Capability to remove extensively covered clouds.	Inability to reconstruct cloud-covered areas without complementary temporal information.
		Long et al. [114], 2021	The visualization of the restored area is excellent.	Poorer performance with significant land cover changes.
		Stucker et al. [115], 2023	Capable of restoring cloud-covered areas in continuous time phases.	Relies on high-quality cloud and cloud shadow masks.
		Lin et al. [116], 2021	Capable of restoring textures in different scenes.	Poor performance for complex structure textures.
	Model-	Ji et al. [117], 2022	Production of smoother restoration results.	Poor shadow removal effect.
	driven	Tu et al. [118], 2023	Effective restoration of detailed textures.	Poor performance with heavy cloud cover.
		Jiang et al. [119], 2023	Capable of restoring complex texture structures.	Poor visual effect of cloud removal result.
		Wang et al. [120], 2023	Detail preservation in restoration results.	Poor restoration effect in complex texture scenes.
Blind		Chen et al. [121], 2024	Minimization of visual artifacts.	Limited generalization capability.
Technique		Jiang et al. [122], 2022	Capable of simultaneously processing three- phase cloud cover images.	Limited reconstruction capability for different seasons.
	Data- driven	Ebel et al. [123], 2023	Excellent color representation in detail restoration.	Poor performance in visual effect.
		Yang et al. [124], 2023	Good restoration performance of landscape details.	Need for improvement in finer detail restoration.
		Zi et al. [125], 2024	Excellent performance in color consistency.	Influence by discrete noise.
		Zhou et al. [126], 2025	Mitigated interference noise.	High parameter volume.
		Sebastianelli et al. [127], 2022	Capable of handling all weather conditions.	Poor performance under high cloud coverage.
	SAR Fusion	Wang et al. [128], 2023	Outstanding performance in spectral preservation.	Poor performance on thick clouds.

TABLE III
SUMMARY OF TYPICAL MULTITEMPORAL-BASED METHODS

images to eliminate clouds and reconstruct the cloudy regions, demonstrating a marked advantage in handling dense and extensive clouds. The existing approaches for multitemporal cloud removal can be generally divided into nonblind and blind methods, based on the necessity of employing a cloud mask, as shown in Table III.

1) Multitemporal NonBlind Technique: As cloud detection technology in ORS images has progressed, it is possible to acquire extensive masks that identify regions affected by cloud contamination [131]. Nonblind multitemporal cloud removal methods utilize these masks, either provided or obtained through prior cloud detection, to delineate the impaired areas and subsequently employ the complementary information from cloud-free regions across various time phases to reconstruct the underlying data [110]. This methodology ensures spectral consistency in cloud-free regions, guided by the mask.

In the early stages of nonblind multitemporal cloud removal, methods directly filled or replaced cloudy areas with similar information from cloud-free regions in multiple time phases. Techniques such as global optimization [132], Markov random fields energy model [133], dictionary learning [134], weighted regression model [135], and sparse representation [136] were used to find the closest matching cloudy patches within the multitemporal images. Early approaches relied on a straightforward strategy of filling in cloudy areas using similar information from multitemporal images at the same location, neglecting the temporal variations of the materials within the multitemporal images. In addition, these methods presupposed that the corresponding regions in the auxiliary multitemporal images were free of clouds, which often led to structural and spectral inaccuracies in the reconstructed cloud-free images.

Considering the spectral disparities among multitemporal images, methodologies grounded in low-rank modeling, tensor decomposition, or sparse representation have been developed to distill low-rank and sparse features from the multitemporal images for restoring cloudy areas. Such approaches can effectively capture the interdependencies among the multitemporal images,

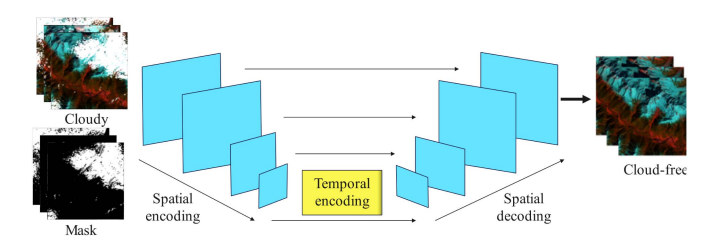


Fig. 6. Commonly applied U-Net architecture in multitemporal nonblind cloud removal methods [117]. The architecture includes a spatial encoder, a temporal encoder, and a spatial decoder, which are used to extract spatial features, extract key temporal features, and reconstruct cloud-free images, respectively.

yielding more precise restoration outcomes than the traditional similarity-based replacement techniques. Furthermore, hybrid approaches leverage low-rank tensor reconstruction to uncover intrinsic structural features across multiple time phases and integrate deep priors to capture contextual information [108], [137], [138], [139]. These low-rank modeling, tensor decomposition, and sparse representation are collectively known as model-driven methods, which do not require cloud-free regions in the multitemporal auxiliary images. However, they presuppose a minimal ground change, which is challenging to fulfill in practical scenarios. Like the model-driven methods discussed in Section II-A1, these approaches also encounter issues related to parameter tuning and sensitivity to outliers.

The advent of deep learning has significantly advanced this field, with neural networks employed to represent multitemporal ORS images and to discern the mapping between multitemporal cloudy regions and clear regions. For instance, end-to-end CNNs have been effectively utilized to learn the relationship between missing data and the auxiliary information from multiple time phases [140], [141], [142]. Stucker et al. [117] presented another U-Net model for cloud removal. The commonly applied U-Net architecture as shown in Fig. 6. Data-driven approaches are capable of capturing the nuances of temporal series variations, which can result in more precise cloud removal. Nevertheless, they encounter the pervasive challenges associated with deep learning: The necessity for an ample training dataset to ensure robust generalization, and the substantial demands on data resources, hardware, and training time.

In summary, if a cloud mask has been preidentified, employing multitemporal nonblind cloud removal techniques can more precisely leverage auxiliary data from multiple time phases to reconstruct cloudy areas. These methods concentrate solely on the regions of missing data, establishing a connection between these areas and the multitemporal images, thereby enabling the reconstruction of promising outcomes [119]. However, the intricacy of clouds poses a significant challenge to the accurate manual annotation or automatic detection of cloud masks. Consequently, if the cloud mask is not known beforehand or if the precision of cloud detection is suboptimal, the efficacy of these methods may be compromised or the quality may be markedly diminished. Furthermore, while these methods can address the temporal spectral variations presented in multitemporal images, the temporal changes in the structural composition of the ground features remain an open question.

2) Multitemporal Blind Technique: To mitigate the dependence on masks, numerous high-performing blind methods have been introduced. These multitemporal blind techniques eliminate clouds without the provision of a predefined cloud mask and without the prerequisite of a preliminary cloud detection process [110]. They are adept at multitemporal dehazing in noncomplementary scenarios and are particularly effective in addressing extensive regions of dense cloud cover. In addition, the absence of a mask requirement simplifies the integration of multitemporal and multisource methodologies.

Model-driven blind methods for multitemporal images utilize models such as sparse representation [143] or matrix factorization [144] to forge connections between multitemporal images or to distill key features for restoration. These approaches enable the integration of cloud detection within the cloud removal process, allowing for the simultaneous identification and clearance of cloud masks. Similar to multitemporal nonblind method, these techniques rely heavily on the quality of cloudfree multitemporal auxiliary data and require clear images at multiple times as supplementary information. Recently, new methodologies have emerged that do not impose the condition of complete clarity and cloudlessness for multitemporal auxiliary data. Tu et al. [120] used a weighted nuclear norm to adaptively describe low-rank attributes with group sparsity constraints to characterize the sparse nature of cloud component difference maps. While the above methods do not mandate a full set of clear images across time, they generally require a collection of multitemporal images with diverse cloud coverage, typically more than two, to act as auxiliary inputs. Approaches that characterize data through sparsity or low-rank features risk undermining the intrinsic high-dimensional structures and disregard multitemporal semantic correlations, showing a heightened sensitivity to anomalies [119]. In addition, the efficacy of model-driven cloud removal is contingent upon the parameters of representational dimensions, regularization, and prior knowledge, as various image scenes may call for distinct optimal settings [143]. Some alternative methods explore the integration of neural networks to distill multitemporal prior knowledge, aiming to amplify the potency of the prior information inherent in model-driven techniques. Nevertheless, there is a dearth of research that specifically integrates data-driven and modeldriven approaches, and this hybrid approach remains largely unexplored [123].

The data-driven multitemporal blind cloud removal techniques leverage deep neural networks to discern the complex mappings between multitemporal cloudy images and the desired cloud-free images. This conversion process from cloudy to cloud-free is based on the network's ability to capture complex relationships. Compared to model-driven approaches, these data-driven methods excel in extracting both global and local features across multiple temporal datasets, thereby yielding superior cloud removal outcomes. However, studies that specifically integrate data-driven and model-driven approaches for cloud removal tasks are relatively scarce, and the potential of such hybrid methods remains largely untapped. The challenge of information fusion without an effective selection mechanism is critical in data-driven multitemporal blind cloud removal

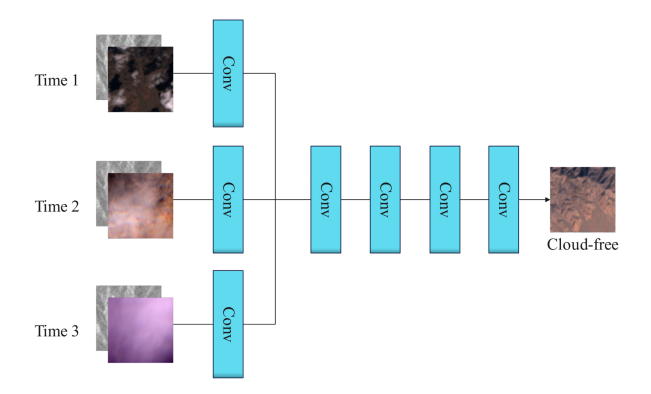


Fig. 7. Widely used CNN structure in multitemporal blind cloud removal methods [145]. The structure processes time information and extracts features through convolutional blocks, and removes clouds in a sequence-to-sequence manner.

methods. Neglecting these mechanisms poses a risk of cloud interference or redundant data, which could compromise the efficient use of cloud-free regions and reduce overall performance [126]. Nevertheless, neither model-driven nor data-driven approaches have fully addressed the impact of temporal variations in multitemporal data of terrestrial surfaces.

To mitigate the effects of these temporal changes, some research has merged multitemporal cloud removal with SAR data fusion techniques. For example, approaches that employ X-fork Genetic Algorithms or Conditional GAN (cGAN) integrate multitemporal and SAR images into an end-to-end generator designed to produce cloud-free images [146], [147]. Ebel et al. [145] released a multitemporal decloud dataset containing paired ORS and SAR images, and designed a 3-D CNN and a sequence translation model. The widely used CNN structure as shown in Fig. 7. The essence of the challenge for hybrid models is the integration of multitemporal and multisource data without the benefit of prior information. Although these hybrid techniques can leverage the advantages of both methodologies, they also risk obscuring the distinct weaknesses inherent to each. A case in point is the speckle noise commonly found in SAR image. Likewise, while data-driven cloud removal is adept at eliminating clouds and can be highly effective, it is not without its drawbacks, including prolonged training durations, suboptimal cloud clearance, and potential color distortion [119].

In summary, the hallmark of multitemporal blind methods—their independence from reliance on masks—eases the workload of manual annotation and reduces the cloud removal implications stemming from inaccuracies in mask detection. These approaches exhibit superior advantages in hybrid model-driven scenarios, as well as in the integration of multisource, multispectral, and spatial data. Consequently, multitemporal blind methods have emerged as a prominent trend in the field of cloud removal for ORS images in recent years.

3) Current Issues and Future Prospects: Multitemporal cloud removal techniques, recognized for their efficacy in addressing dense and extensive cloud coverage, have seen widespread application in the cloud removal of satellite ORS and aerial images. However, the prerequisite for these methods is the acquisition of multitemporal images from a consistent vantage

point, and instrumental discrepancies can lead to geometric misalignment and registration inaccuracies [114]. Furthermore, an overly brief sampling interval may result in similar cloud patterns across images, diminishing the availability of auxiliary information. In contrast, an extended interval could see changes in terrestrial and spectral properties that adversely affect the restoration process [148].

Looking ahead, the integration of multitemporal blind cloud removal methods with the strengths of both model-driven and data-driven strategies is anticipated to expand their applications. As large-scale modeling technologies progress and hardware capabilities advance, more sophisticated cloud removal approaches that leverage multitemporal, multisource, and multispectral data, while simultaneously capturing temporal, spectral, and spatial correlations, are poised to significantly enhance cloud removal outcomes. Despite the promise of hybrid methodologies, challenges persist in harnessing complementary information across spatial, spectral, and temporal domains, particularly due to variations in multisource images and differences in spatial resolution [144].

III. PERFORMANCE EVALUATIONS AND DISCUSSIONS

A. Experiment Preparation

- 1) Datasets: To illustrate the cloud removal capabilities of the methods, we performed comparative performance experiments on typical datasets tailored to each method. Typical datasets used are as follows:
 - a) The remote sensing image cloud removing (RICE) dataset [149], a benchmark for single-image cloud removal, comprises two subsets: RICE1 and RICE2, with each image dimensioned at 512 × 512 pixels. RICE1 encompasses 500 pairs of cloudy and clear images, emulating light cloud cover through artificially generated semitransparent haze. RICE2, in contrast, fabricates 736 cloud-mask-clear image pairs to mimic dense cloud coverage.
 - b) The sentinel-1/2 multispectral cloud removal (SEN12MS-CR) [150], a widely recognized multimodal cloud removal dataset, includes 13-band ORS image pairs and 2-band SAR images. It encompasses 122 218 paired samples, each 256×256 pixels in size, capturing four seasons across 175 distinct geographical locations.
 - c) The SEN12MS-CR Time Series (SEN12MS-CR-TS) dataset [145], designed for multitemporal cloud removal, spans 53 distinct geographical locations. It encompasses 15 578 paired samples, each sample includes 30 different temporal phases of 13-band ORS image pairs and 2-band SAR images, segmented into numerous 256 × 256 pixel blocks.
- 2) Metrics: To evaluate the effectiveness of these methods more comprehensively on test datasets, we utilized four standard cloud removal evaluation metrics [151]. Evaluation metrics used are as follows:
 - a) The structural similarity index (SSIM) gauges the similarity in structure between the reconstructed and the clear image, thereby evaluating the veracity of the reconstructed image. It encapsulates structural information as an

TABLE IV COMPARISON RESULTS OF AVERAGE SSIM/PSNR/CIEDE/LPIPS ON BENCHMARK DATASETS

Methods	RICE1			RICE2				
Methods	SSIM	PSNR	RMSE	LPIPS	SSIM	PSNR	RMSE	LPIPS
DCP [25]	0.86	17.17	10.363	0.09	0.626	17.06	9.64	0.417
FFA [150]	0.94	28.59	7.085	0.045	0.901	32.36	6.635	0.112
Trinity-Net [151]	0.943	29.24	6.804	0.039	0.888	29.83	6.533	0.145
PSMB-Net [152]	0.934	29.9	6.396	0.043	0.9	31.77	5.554	0.114
DCIL [153]	0.957	31.61	5.481	0.033	0.903	33.09	5.113	0.116
DehazeFormer [154]	0.956	32.39	5.364	0.037	0.908	34.76	4.587	0.122
EMPF [155]	0.954	31.79	5.733	0.027	0.899	33.49	5.002	0.115
MABDT-DW [36]	0.957	31.88	5.572	0.032	0.907	34.15	4.69	0.112
ConvIR-B [156]	0.957	31.69	5.621	0.04	0.911	34.18	4.725	0.114
ChaIR [157]	0.959	32.41	5.294	0.038	0.91	34.6	4.668	0.108

amalgamation of luminance, contrast, and texture. An SSIM value nearing 1 signifies that the structural attributes of the reconstructed image closely mirror those of the clear image.

- b) The peak signal-to-noise ratio (PSNR) quantifies image quality by calculating the mean square error. A higher PSNR indicates less distortion in the reconstructed image.
- c) The root mean square error (RMSE) serves as an error metric, determining the root mean square error in pixel intensities between the reconstructed and clear images. A lower RMSE indicates a higher fidelity of the reconstructed image with less perceptible distortion.
- d) The learned perceptual image patch similarity (LPIPS) captures detailed information that the human visual system focuses on, demonstrating strong applicability in practical scenarios. Aligning closely with human perception, a lower LPIPS value signifies greater image authenticity.

B. Experimental Results and Analysis

In the subsequent analysis, we assessed the cloud removal performance of the methods across various scenarios and cloud cover levels using a blend of qualitative and quantitative evaluations. Ten single-image methods were trained for 1000 iterations using the same datasets. Similarly, four multimodal and three multitemporal methods were trained for 60 iterations using the same dataset. All comparison experiments were conducted on a platform equipped with an Intel i5-10400F processor and an NVIDIA GeForce RTX 4070 GPU. The remaining parameters of each method were kept consistent with those in the original papers.

We selected ten effective single-image methods for comparison: DCP [25], feature fusion attention (FFA) [152], Trinity-Net [153], partial siamese with multiscale bicodec network (PSMB-Net) [154], dynamic collaborative inference learning (DCIL) [155], Dehazing Transformer (DehazeFormer) [156], encoder-free multiaxis physics-aware fusion (EMPF) [157], multiscale attention boosted deformable transformer-depth wise (MABDT-DW) [36], channel interactions for image restoration (ChaIR) [159], and revitalizing convolutional network for image restoration (ConvIR-B) [158]. Among them, ChaIR currently stands out as a superior single-image approach for cloud removal. As depicted in Table IV, both methods exhibit outstanding performance on all evaluation metrics, with particular excellence noted in brightness, spectral fidelity, and visual

TABLE V
AVERAGE METRIC RESULTS OF MULTIMODAL-BASED AND
MULTITEMPORAL-BASED METHODS ON SEN12MS-CR-TS

Category	Method	SSIM	PSNR	RMSE	LPIPS
	DSen2-CR [158]	0.881	29.94	7.967	0.307
Multimodal	GLF-CR [85]	0.886	30.16	6.225	0.283
Multimodai	TASANet	0.894	30.93	5.826	0.223
	DiffCR [89]	0.895	31.13	5.387	0.204
	U-TAE [159]	0.879	29.12	8.269	0.325
Multitemporal	CR-TS Net [143]	0.882	29.72	7.823	0.314
	UnCRtainTS [123]	0.892	30.27	5.913	0.247

perceptual authenticity. As shown in Fig. 8, these methods deliver satisfactory outcomes in scenarios with light cloud cover and haze. Nevertheless, in scenes characterized by denser and thicker cloud layers, issues such as artifacts and distortions become evident. While single-image cloud removal techniques are capable of addressing semitransparent clouds, their effectiveness is compromised when confronted with scenarios where thick clouds completely block the ground features, due to the limited information that can be gleaned from a single image. This limitation inherently restricts the cloud removal capabilities in such instances.

As depicted in Table V and Fig. 9, the exemplary cloud removal outcomes of multimodal approaches include deep sentinel-2 cloud removal (DSen2-CR) [160], global-local fusion cloud removal (GLF-CR) [86], tied and anchored stereo attention network (TASANet), and diffusion cloud removal (DiffCR) [90]. Among them, DiffCR currently stands out as a superior multimodal approach for cloud removal. Compared to GLF-CR, DiffCR demonstrates higher performance in structural and textural restoration metrics, along with reduced distortion in both brightness and spectral fidelity. Both techniques exhibit commendable thick cloud removal capabilities across different levels of cloud coverage. DSen2-CR retained the original input but converted some parts of the image into artifacts. GLF-CR is plagued by residual cloud shadows and artifact issues. TASANet employs multiscale feature extraction to mitigate artifact generation. DiffCR significantly alleviates the artifact phenomenon but introduces extra noise. These multimodal techniques are designed to incorporate supplementary SAR data, enabling the recovery of textures obscured by dense cloud. Nonetheless, the presence of SAR speckle noise disrupts the fusion process, leading to the persistence of artifacts in the final declouded images.

The representative cloud removal outcomes of multitemporal approaches are depicted in Table V and Fig. 9, featuring U-net with Temporal Attention Encoder (U-TAE) [161], cloud removal satellite time (CR-TS Net) [145], and uncertainty quantification for cloud removal in optical satellite time series (UnCR-tainTS) [125]. Among them, UnCRtainTS currently stands out as a superior multitemporal approach for cloud removal. These methods leverage supplementary data from different temporal to proficiently restore information from dense cloud regions. While both approaches have demonstrated success in structural and textural restoration, there remains scope for enhancement in fidelity and visual authenticity. U-TAE collapses the time dimension into

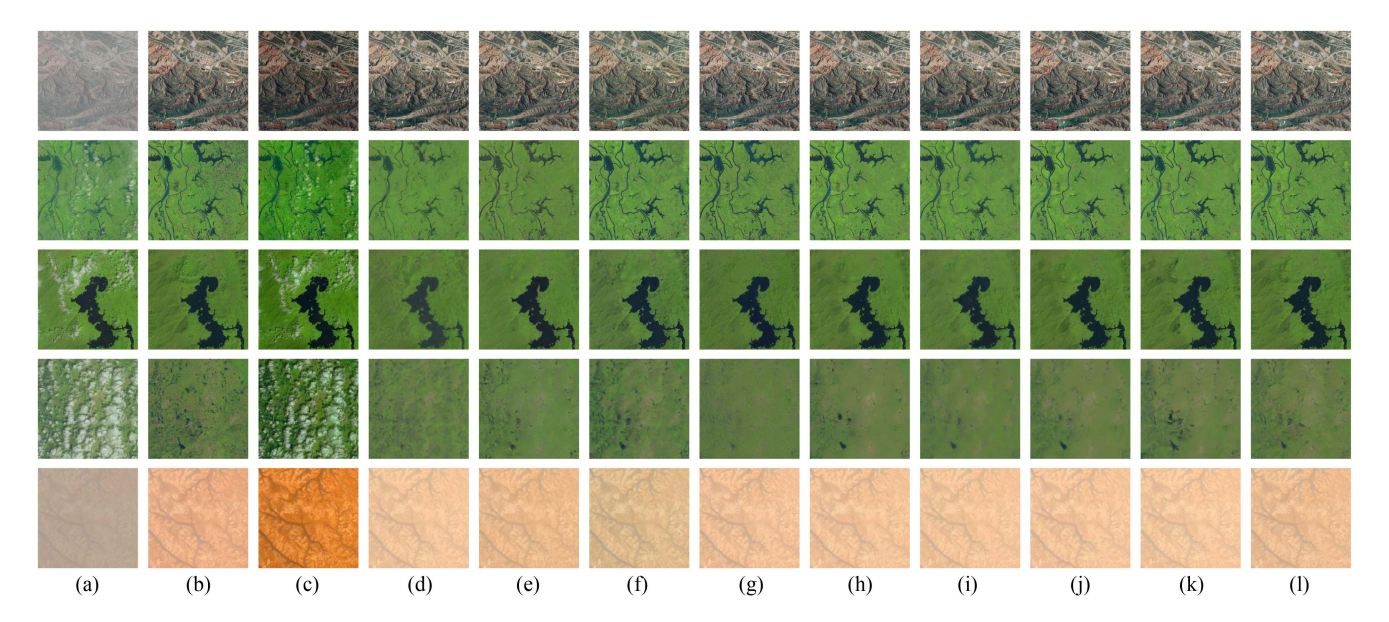


Fig. 8. Visualization results of single-image methods on RICE. From left to right are (a) cloudy ORS images, (b) cloud-free ORS images, (c) results of DCP, (d) results of FFA, (e) results of Trinity-Net, (f) results of PSMB-Net, (g) results of DCIL, (h) results of DehazeFormer, (i) results of EMPF, (j) results of MABDT-DW, (k) results of ConvIR-B, and (l) results of ChaIR.

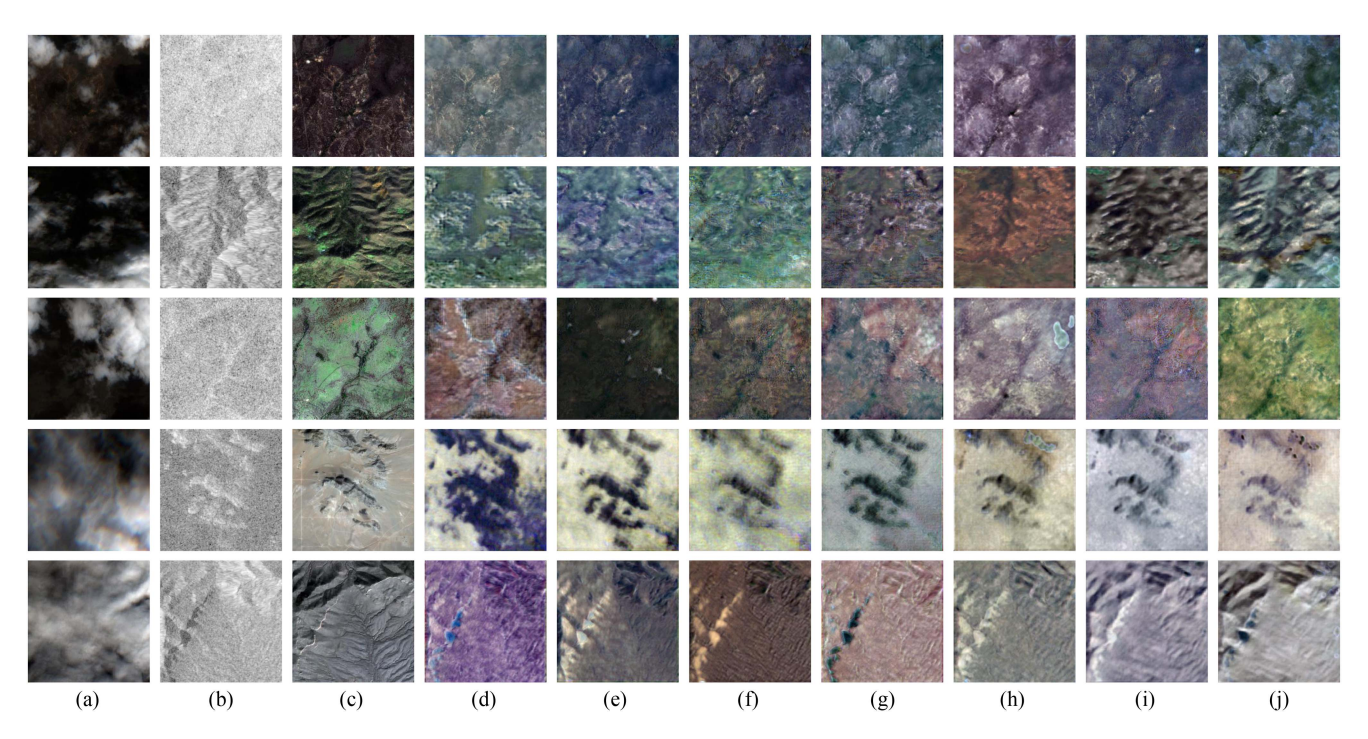


Fig. 9. Visualization results of multitemporal methods on SEN12MS-CR-TS. From left to right are (a) cloudy ORS images, (b) SAR images, (c) cloud-free ORS images, (d) results of U-TAE, (e) results of DSen2-CR, (f) results of CR-TS Net, (g) results of GLF-CR, (h) results of UnCRtainTS, (i) results of TASANet, and (j) results of DiffCR.

a single mapping. CR-TS Net employs a sequence-to-sequence network to diminish noise, whereas UnCRtainTS incorporates uncertainty predictions into its loss function, leading to more authentic color recovery and finer textural details. Upon examining the declouded outcomes, it is evident that the incorporation of multitemporal land cover variations introduces persistent artifacts and distortions.

C. Discussions

Combining the experimental results with the methods review reveals that various cloud removal techniques exhibit unique strengths when addressing different types of cloud coverage and image information. Single-image methods excel in scenarios with haze and semitransparent clouds by capitalizing on the current cloud areas and adjacent similar features. They are straightforward and efficient, eliminating the need for extra auxiliary data collection and alignment preprocessing. In contrast, multimodal, multitemporal methods shine in thick cloud scenarios by tapping into additional structural or historical information. Researchers can opt for the most appropriate method among these three categories, contingent upon their hardware and data conditions, to either remove clouds or reduce their impact, thus improving the precision of subsequent sophisticated tasks. Nonetheless, it is imperative to acknowledge the constraints inherent in these methods, such as

- 1) Data Pairing Challenge: Deep learning approaches often require cloud-free and cloudy image pairs of the same size and resolution at the same location for guiding model training. However, in real-world scenarios, capturing paired ORS images from the same location at the same time is impractical. Even with minimal time intervals, variations in terrain and lighting conditions are unavoidable. Confronted with this predicament, researchers often utilize cloud-free images combined with cloud masks to synthetically generate cloudy images. These synthetic image pairs tend to exhibit substantial generalization errors, significantly diminishing their effectiveness in cloud removal when applied to actual cloudy images. Furthermore, multimodal and multitemporal methods demand not only the alignment of cloud-free and cloudy images but also the precise registration and matching of SAR and multitemporal images, which significantly amplifies the complexity of data preprocessing.
- 2) Complexity of Cloud Features: The complexity of cloud features is manifested in their irregular shapes, uneven concentrations, and nonuniform distributions. These characteristics exacerbate the inaccuracy of feature extraction or information fusion in cloud removal models. Consequently, after cloud removal operations, cloud regions may still exhibit lingering blur, distortion, artifacts, and detail distortion. The most effective cloud removal techniques currently rely on neural networks, but these can lead to the loss of detailed features due to their fixed-size convolutions and pooling operations. Moreover, single-image cloud removal is constrained by information limitations, which hinder its effectiveness in dealing with dense clouds. In addition, SAR fusion introduces extra speckle noise, while multitemporal methods ignore the temporal changes in the landscape.
- 3) Inadequate Information Utilization: Constrained by computational and storage resources, some research discard multispectral information by converting ORS images into RGB three-channel images that are perceptible to the human eye. Some studies discard long temporal sequences, preserving only a select few data points. Such information compression leads to a substantial loss of detail, thereby constraining the efficacy of cloud removal models. Thus, preserving essential information for cloud removal within the constraints of limited resources poses a significant challenge.

The aforementioned challenges continue to be focal points in ongoing research and are critical issues that demand immediate attention. Potential improvements to key technologies and prospective research avenues for addressing these issues can be encapsulated as follows:

1) To address the challenge of data pairing, cloud detection and segmentation models can be employed to extract cloudy

- features, synthesizing more datasets that closely resemble real-world scenarios. Another approach is to integrate cloud detection and segmentation models with multitask learning frameworks to remove cloud in a concurrent process. Moreover, the model's generalization capabilities can be augmented by employing unsupervised, semisupervised, or weakly supervised learning techniques. For example, GANs can be applied by treating cloudy images as the source domain and cloud-free images as the target domain, thereby generating cloud-free images from cloudy images. In addition, the development of robust, adaptive methods in the frequency domain or model-based approaches that do not rely on labels presents another strategy. Lastly, combining artificially synthesized paired datasets with real-world unpaired datasets and leveraging semisupervised or weakly supervised learning mechanisms is also a viable solution to this issue.
- 2) To tackle the problem of incomplete cloud removal, a model design perspective is essential. While many attention mechanisms and multiscale strategies can indeed focus on the characteristics of complex cloudy regions, they often fail to adequately attend to faint ground signals, resulting in a lack of capability to extract fine local details. Enhancing the attention or extraction of local high-frequency texture features could potentially promote the recovery of more details. Moreover, information fusion should not merely be a matter of concatenation and attention; instead, it should involve more complementary cross-modal interactions. It is also important to emphasize the high-frequency information from SAR data and to mitigate the effects of noise.
- 3) To address the issue of underutilized information, future hybrid methodologies have the potential to significantly improve cloud removal capabilities. For instance, in hybrid model-driven and data-driven methods, the training process can be guided by physical models. Integrating various cloud removal models is anticipated to elevate the overall accuracy. In addition, by combining single-image, multitemporal, multispectral, and SAR data, there is a promising prospect for the development of more robust multimodal, multitemporal fusion methods. Training large-scale cloud removal models on extensive distributed datasets to fully leverage ORS data. Furthermore, adopting lightweight design principles to minimize the extraction of redundant information and reduce model complexity is also essential.

IV. CONCLUSION

The study of cloud removal technologies has become increasingly significant in bolstering the quality of ORS images and increasing its usage rate. This article begins with a comprehensive review and categorization of existing cloud removal techniques, which are categorized into the following main categories: single-image, multimodal, and multitemporal. Each category possesses distinct advantages and is suited to different scenarios, encompassing key technologies such as physical modeling, deep learning, multispectral analysis, and SAR fusion. Comparative experiments on benchmark datasets were subsequently conducted to further evaluate the cloud removal efficacy of these methods. The article concludes with a comprehensive discussion of the challenges impeding these techniques and proposes potential corrective measures.

Several significant initiatives to improve cloud removal capabilities are anticipated to garner extensive interest. These endeavors include the use of unpaired learning mechanisms to bolster the models' generalization ability and the integration of multitask learning frameworks to establish a more holistic processing approach. SAR fusion also aims to develop models that are able to extract or highlight high-frequency texture features, thereby mitigating the impact of speckle noise. In addition, there is a growing interest in exploring hybrid models, especially those with multimodal and multitemporal fusion. The combination of model-driven and data-driven strategies is also emphasized to further improve the models' generalization capabilities. Lastly, the utilization of complementary information across spatial, spectral, and temporal domains is highlighted to mitigate the impact of texture variations.

REFERENCES

- M. Li, Q. Xu, J. Guo, and W. Li, "DecloudNet: Cross-patch consistency is a nontrivial problem for thin cloud removal from wide-swath multispectral images," *IEEE Trans. Geosci. Remote Sens.*, vol. 62, 2024, Art. no. 5407614.
- [2] Y. Sun, C.-K. Tang, and Y.-W. Tai, "Semantic image matting," in Proc. IEEE/CVF Conf. Comput. Vis. Pattern Recognit. (CVPR), 2021, pp. 11115–11124.
- [3] A. Golts, D. Freedman, and M. Elad, "Unsupervised single image dehazing using dark channel prior loss," *IEEE Trans. Image Process.*, vol. 29, pp. 2692–2701, 2019.
- [4] H. Lyu and J. Qian, "Thin cloud removal based on the sorted slow feature analysis for multispectral remotely sensed imagery," in *Proc. IEEE Int. Geosci. Remote Sens. Symp.*, 2023, pp. 3776–3779.
- [5] X. Zhang, W. Yu, M.-O. Pun, and W. Shi, "Cross-domain landslide mapping from large-scale remote sensing images using prototype-guided domain-aware progressive representation learning," *ISPRS J. Photogram-metry Remote Sens.*, vol. 197, pp. 1–17, 2023.
- [6] X. Ma, X. Zhang, Z. Wang, and M.-O. Pun, "Unsupervised domain adaptation augmented by mutually boosted attention for semantic segmentation of VHR remote sensing images," *IEEE Trans. Geosci. Remote Sens.*, vol. 61, 2023, Art. no. 5400515.
- [7] Q. Wang, L. Wang, X. Zhu, Y. Ge, X. Tong, and P. M. Atkinson, "Remote sensing image gap filling based on spatial-spectral random forests," *Sci. Remote Sens.*, vol. 5, 2022, Art. no. 100048.
- [8] J. Liu, B. Pan, and Z. Shi, "Cascaded memory network for optical remote sensing imagery cloud removal," *IEEE Trans. Geosci. Remote Sens.*, vol. 62, 2024, Art. no. 5613611.
- [9] S. Khan, Z. Pirani, T. Fansupkar, and U. Maghrabi, "Shadow removal from digital images using multi-channel binarization and shadow matting," in *Proc. 3rd Int. Conf. I-SMAC (IoT Soc. Mobile Analytics Cloud)* (*I-SMAC*), IEEE, 2019, pp. 723–728.
- [10] M. Xu, X. Jia, and M. Pickering, "Automatic cloud removal for landsat 8 OLI images using cirrus band," in *Proc. 2014 IEEE Geosci. Remote Sens. Symp.*, IEEE, 2014, pp. 2511–2514.
- [11] X. Meng, H. Shen, Q. Yuan, H. Li, L. Zhang, and W. Sun, "Pansharpening for cloud-contaminated very high-resolution remote sensing images," *IEEE Trans. Geosci. Remote Sens.*, vol. 57, no. 5, pp. 2840–2854, May 2019.
- [12] R. Bamler, "Principles of synthetic aperture radar," Surveys Geophys., vol. 21, pp. 147–157, 2000.
- [13] O. Ghozatlou and M. Datcu, "Hybrid GAN and spectral angular distance for cloud removal," in *Proc. IEEE Int. Geosci. Remote Sens. Symp.*, 2021, pp. 2695–2698.
- [14] I. Gladkova, M. D. Grossberg, F. Shahriar, G. Bonev, and P. Romanov, "Quantitative restoration for MODIS band 6 on aqua," *IEEE Trans. Geosci. Remote Sens.*, vol. 50, no. 6, pp. 2409–2416, Jun. 2012.
- [15] W. Yu, X. Zhang, and M.-O. Pun, "Cloud removal in optical remote sensing imagery using multiscale distortion-aware networks," *IEEE Geosci. Remote Sens. Lett.*, vol. 19, 2022, Art. no. 5512605.

- [16] M. Qin, F. Xie, W. Li, Z. Shi, and H. Zhang, "Dehazing for multispectral remote sensing images based on a convolutional neural network with the residual architecture," *IEEE J. Sel. Topics Appl. earth Observ. Remote Sens.*, vol. 11, no. 5, pp. 1645–1655, May 2018.
- [17] J. Jia et al., "GLTF-net: Deep-learning network for thick cloud removal of remote sensing images via global–local temporality and features," *Remote Sens.*, vol. 15, no. 21, 2023, Art. no. 5145.
- [18] J. Sui, Y. Ma, W. Yang, X. Zhang, M.-O. Pun, and J. Liu, "Diffusion enhancement for cloud removal in ultra-resolution remote sensing imagery," *IEEE Trans. Geosci. Remote Sens.*, vol. 62, 2024, Art. no. 5405914.
- [19] C.-H. Lin, K.-H. Lai, Z.-B. Chen, and J.-Y. Chen, "Patch-based information reconstruction of cloud-contaminated multitemporal images," *IEEE Trans. Geosci. Remote Sens.*, vol. 52, no. 1, pp. 163–174, Jan. 2014.
- [20] X. Jin et al., "RFE-VCR: Reference-enhanced transformer for remote sensing video cloud removal," ISPRS J. Photogrammetry Remote Sens., vol. 214, pp. 179–192, 2024.
- [21] Q. Xiong, G. Li, X. Yao, and X. Zhang, "SAR-to-optical image translation and cloud removal based on conditional generative adversarial networks: Literature survey, taxonomy, evaluation indicators, limits and future directions," *Remote Sens.*, vol. 15, no. 4, 2023, Art. no. 1137.
- [22] G. Y. Lee, J. Chen, T. Dam, M. M. Ferdaus, D. P. Poenar, and V. N. Duong, "Dehazing remote sensing and UAV imagery: A review of deep learning, prior-based, and hybrid approaches," 2024, arXiv:2405.07520.
- [23] W. Li, Y. Li, D. Chen, and J. C.-W. Chan, "Thin cloud removal with residual symmetrical concatenation network," *ISPRS J. Photogrammetry Remote Sens.*, vol. 153, pp. 137–150, 2019.
- [24] Y. Zhang, B. Guindon, and J. Cihlar, "An image transform to characterize and compensate for spatial variations in thin cloud contamination of landsat images," *Remote Sens. Environ.*, vol. 82, no. 2/3, pp. 173–187, 2002.
- [25] K. He, J. Sun, and X. Tang, "Single image haze removal using dark channel prior," *IEEE Trans. Pattern Anal. Mach. Intell.*, vol. 33, no. 12, pp. 2341–2353, Dec. 2011.
- [26] G. Hu, X. Li, and D. Liang, "Thin cloud removal from remote sensing images using multidirectional dual tree complex wavelet transform and transfer least square support vector regression," *J. Appl. Remote Sens.*, vol. 9, no. 1, 2015, Art. no. 095053.
- [27] M. Wan and X. Li, "Removing thin cloud on single remote sensing image based on SWF," in *Proc. IEEE Int. Conf. Online Anal. Comput. Sci.* (ICOACS), IEEE, 2016, pp. 397–400.
- [28] S. Zhao and S. Dai, "Automated cloud removal and filling in optical remote sensing images," in *Proc. Int. Conf. Virtual Reality Visual. (ICVRV)*, IEEE, 2016, pp. 292–297.
- [29] M. Xu, X. Jia, M. Pickering, and S. Jia, "Thin cloud removal from optical remote sensing images using the noise-adjusted principal components transform," *ISPRS J. Photogrammetry Remote Sens.*, vol. 149, pp. 215–225, 2019.
- [30] S. Shi, Y. Zhang, X. Zhou, and J. Cheng, "A novel thin cloud removal method based on multiscale dark channel prior (MDCP)," *IEEE Geosci. Remote Sens. Lett.*, vol. 19, 2021, Art. no. 1001905.
- [31] C. Zhang, P. Yi, Y. Liu, L. Ma, W. Hu, and J. Wu, "Thin cloud correction method for visible remote sensing images using a spectral transformation scheme," *GIScience Remote Sens.*, vol. 60, no. 1, 2023, Art. no. 2196133.
- [32] Q. Yang, G. Wang, Y. Zhao, X. Zhang, G. Dong, and P. Ren, "Multi-scale deep residual learning for cloud removal," in *Proc. IEEE Int. Geosci. Remote Sens. Symp.*, IEEE, 2020, pp. 4967–4970.
- [33] X. Wen, Z. Pan, Y. Hu, and J. Liu, "An effective network integrating residual learning and channel attention mechanism for thin cloud removal," *IEEE Geosci. Remote Sens. Lett.*, vol. 19, 2022, Art. no. 6507605.
- [34] Y. Zi, H. Ding, F. Xie, Z. Jiang, and X. Song, "Wavelet integrated convolutional neural network for thin cloud removal in remote sensing images," *Remote Sens.*, vol. 15, no. 3, 2023, Art. no. 781.
- [35] Y. Guo, W. He, Y. Xia, and H. Zhang, "Blind single-image-based thin cloud removal using a cloud perception integrated fast fourier convolutional network," *ISPRS J. Photogrammetry Remote Sens.*, vol. 206, pp. 63–86, 2023.
- [36] J. Ning, J. Yin, F. Deng, and L. Xie, "MABDT: Multi-scale attention boosted deformable transformer for remote sensing image dehazing," *Signal Process.*, vol. 229, 2024, Art. no. 109768.
- [37] Y. Yan, Y. He, N. Su, G. He, and H. Fu, "PNBT-CR: A cloud removal method for ship detection," *IEEE Geosci. Remote Sens. Lett.*, vol. 21, 2024, Art. no. 1501905.

- [38] B. Jiang et al., "FDT-Net: Deep-learning network for thin-cloud removal in remote sensing image using frequency domain training strategy," *IEEE Geosci. Remote Sens. Lett.*, vol. 21, 2024, Art. no. 1002405.
- [39] M. Li, Q. Xu, K. Li, and W. Li, "DecloudFormer: Quest the key to consistent thin cloud removal of wide-swath multi-spectral images," *Pattern Recognit.*, vol. 166, 2025, Art. no. 111664.
- [40] T. Toizumi, S. Zini, K. Sagi, E. Kaneko, M. Tsukada, and R. Schettini, "Artifact-free thin cloud removal using GANs," in *Proc. IEEE Int. Conf. Image Process. (ICIP)*, IEEE, 2019, pp. 3596–3600.
- [41] J. Li et al., "Thin cloud removal in optical remote sensing images based on generative adversarial networks and physical model of cloud distortion," *ISPRS J. Photogrammetry Remote Sens.*, vol. 166, pp. 373–389, 2020.
- [42] H. Pan, "Cloud removal for remote sensing imagery via spatial attention generative adversarial network," 2020, *arXiv:2009.13015*.
- [43] X. Wen, Z. Pan, Y. Hu, and J. Liu, "Generative adversarial learning in YUV color space for thin cloud removal on satellite imagery," *Remote Sens.*, vol. 13, no. 6, 2021, Art. no. 1079.
- [44] Y. Zhao, S. Shen, J. Hu, Y. Li, and J. Pan, "Cloud removal using multimodal GAN with adversarial consistency loss," *IEEE Geosci. Remote Sens. Lett.*, vol. 19, 2021, Art. no. 8015605.
- [45] J. Zhou, X. Luo, W. Rong, and H. Xu, "Cloud removal for optical remote sensing imagery using distortion coding network combined with compound loss functions," *Remote Sens.*, vol. 14, no. 14, 2022, Art. no. 3452.
- [46] J. Liu, W. Hou, X. Luo, J. Su, Y. Hou, and Z. Wang, "SI-SA GAN: A generative adversarial network combined with spatial information and self-attention for removing thin cloud in optical remote sensing images," *IEEE Access*, vol. 10, pp. 114318–114330, 2022.
- [47] D. Ma, R. Wu, D. Xiao, and B. Sui, "Cloud removal from satellite images using a deep learning model with the cloud-matting method," *Remote Sens.*, vol. 15, no. 4, 2023, Art. no. 904.
- [48] P. Singh and N. Komodakis, "Cloud-GAN: Cloud removal for sentinel-2 imagery using a cyclic consistent generative adversarial networks," in *Proc. IEEE Int. Geosci. Remote Sens. Symp.*, IEEE, 2018, pp. 1772–1775.
- [49] Y. Zi, F. Xie, X. Song, Z. Jiang, and H. Zhang, "Thin cloud removal for remote sensing images using a physical-model-based CycleGAN with unpaired data," *IEEE Geosci. Remote Sens. Lett.*, vol. 19, 2021, Art. no. 1004605.
- [50] Y. Mo, C. Li, Y. Zheng, and X. Wu, "DCA-CycleGAN: Unsupervised single image dehazing using dark channel attention optimized CycleGAN," J. Vis. Commun. Image Representation, vol. 82, 2022, Art. no. 103431.
- [51] R. Jaisurya and S. Mukherjee, "AGLC-GAN: Attention-based global-local cycle-consistent generative adversarial networks for unpaired single image dehazing," *Image Vis. Comput.*, vol. 140, 2023, Art. no. 104859.
- [52] H. Ye, H. Xiang, and F. Xu, "Cycle-GAN network incorporated with atmospheric scattering model for dust removal of martian optical images," *IEEE Trans. Geosci. Remote Sens.*, vol. 62, 2024, Art. no. 5633413.
- [53] C. Yu, L. Chen, L. Su, M. Fan, and S. Li, "Kriging interpolation method and its application in retrieval of modis aerosol optical depth," in *Proc.* 19th Int. Conf. Geoinformatics, IEEE, 2011, pp. 1–6.
- [54] X. Zhu, F. Gao, D. Liu, and J. Chen, "A modified neighborhood similar pixel interpolator approach for removing thick clouds in landsat images," *IEEE Geosci. Remote Sens. Lett.*, vol. 9, no. 3, pp. 521–525, May 2012.
- [55] H. Shen, H. Li, Y. Qian, L. Zhang, and Q. Yuan, "An effective thin cloud removal procedure for visible remote sensing images," *ISPRS J. Photogrammetry Remote Sens.*, vol. 96, pp. 224–235, 2014.
- [56] M. He, B. Wang, W. Sheng, K. Yang, and L. Hong, "Thin cloud removal method in color remote sensing image," *Opt. Tech.*, vol. 43, pp. 503–508, 2017.
- [57] J. Ning, Y. Zhou, X. Liao, and B. Duo, "Single remote sensing image dehazing using robust light-dark prior," *Remote Sens.*, vol. 15, no. 4, 2023, Art. no. 938.
- [58] C. Tao, S. Fu, J. Qi, and H. Li, "Thick cloud removal in optical remote sensing images using a texture complexity guided self-paced learning method," *IEEE Trans. Geosci. Remote Sens.*, vol. 60, 2022, Art. no. 5619612.
- [59] K. Zhang, W. Zuo, Y. Chen, D. Meng, and L. Zhang, "Beyond a Gaussian denoiser: Residual learning of deep CNN for image denoising," *IEEE Trans. Image Process.*, vol. 26, no. 7, pp. 3142–3155, Jul. 2017.
- [60] Z. Shao, Y. Pan, C. Diao, and J. Cai, "Cloud detection in remote sensing images based on multiscale features-convolutional neural network," *IEEE Trans. Geosci. Remote Sens.*, vol. 57, no. 6, pp. 4062–4076, Jun. 2019.
- [61] Y. Chen, Z. Cai, J. Yuan, and L. Wu, "A novel dense-attention network for thick cloud removal by reconstructing semantic information," *IEEE J. Sel. Topics Appl. Earth Observ. Remote Sens.*, vol. 16, pp. 2339–2351, 2023

- [62] L. Metz, B. Poole, D. Pfau, and J. Sohl-Dickstein, "Unrolled generative adversarial networks," 2016, arXiv:1611.02163.
- [63] X. Wang, G. Xu, Y. Wang, D. Lin, P. Li, and X. Lin, "Thin and thick cloud removal on remote sensing image by conditional generative adversarial network," in *Proc. IEEE Int. Geosci. Remote Sens. Symp.*, IEEE, 2019, pp. 1426–1429.
- [64] P. Isola, J.-Y. Zhu, T. Zhou, and A. A. Efros, "Image-to-image translation with conditional adversarial networks," in *Proc. IEEE Conf. Comput. Vis. Pattern Recognit.*, 2017, pp. 1125–1134.
- [65] H. Zhang, H. Xu, X. Tian, J. Jiang, and J. Ma, "Image fusion meets deep learning: A survey and perspective," *Inf. Fusion*, vol. 76, pp. 323–336, 2021
- [66] J. Ma, L. Tang, F. Fan, J. Huang, X. Mei, and Y. Ma, "SwinFusion: Cross-domain long-range learning for general image fusion via swin transformer," *IEEE/CAA J. Automatica Sinica*, vol. 9, no. 7, pp. 1200–1217, Jul. 2022.
- [67] L. Tang, Y. Deng, Y. Ma, J. Huang, and J. Ma, "SuperFusion: A versatile image registration and fusion network with semantic awareness," *IEEE/CAA J. Automatica Sinica*, vol. 9, no. 12, pp. 2121–2137, Dec. 2022.
- [68] S. Chen, W. Zhang, Z. Li, Y. Wang, and B. Zhang, "Cloud removal with SAR-optical data fusion and graph-based feature aggregation network," *Remote Sens.*, vol. 14, no. 14, 2022, Art. no. 3374.
- [69] Y. Li, F. Wei, Y. Zhang, W. Chen, and J. Ma, "HS2P: Hierarchical spectral and structure-preserving fusion network for multimodal remote sensing image cloud and shadow removal," *Inf. Fusion*, vol. 94, pp. 215–228, 2023.
- [70] S. Han, J. Wang, and S. Zhang, "Former-CR: A transformer-based thick cloud removal method with optical and SAR imagery," *Remote Sens.*, vol. 15, no. 5, 2023, Art. no. 1196.
- [71] L. Wang et al., "SAR-to-optical image translation using supervised cycle-consistent adversarial networks," *IEEE Access*, vol. 7, pp. 129136–129149, 2019.
- [72] M. Czerkawski et al., "Deep internal learning for inpainting of cloudaffected regions in satellite imagery," *Remote Sens.*, vol. 14, no. 6, 2022, Art. no. 1342.
- [73] J. Cheng, Y. Zhang, X. Zhou, and S. Shi, "A low-rank and sparse constrained dark channel prior for cloud removal in remote sensing image sequence," in *Proc. 2021 IEEE Int. Geosci. Remote Sens. Symp.*, 2021, pp. 3861–3864.
- [74] L. Wang and Q. Wang, "Fast spatial-spectral random forests for thick cloud removal of hyperspectral images," *Int. J. Appl. Earth Observ. Geoinf.*, vol. 112, 2022, Art. no. 102916.
- [75] L. Arp et al., "Training-free thick cloud removal for sentinel-2 imagery using value propagation interpolation," *ISPRS J. Photogrammetry Re*mote Sens., vol. 216, pp. 168–184, 2024.
- [76] Y. Zhang, W. Zhang, J. Zhang, and J. Yin, "Double rank-one prior: Thin cloud removal by visible bands," *IEEE Trans. Geosci. Remote Sens.*, vol. 62, 2024, Art. no. 5622710.
- [77] J. Guo, J. Yang, H. Yue, H. Tan, C. Hou, and K. Li, "RSDehazeNet: Dehazing network with channel refinement for multispectral remote sensing images," *IEEE Trans. Geosci. Remote Sens.*, vol. 59, no. 3, pp. 2535–2549, Mar. 2021.
- [78] Y. Zi, F. Xie, N. Zhang, Z. Jiang, W. Zhu, and H. Zhang, "Thin cloud removal for multispectral remote sensing images using convolutional neural networks combined with an imaging model," *IEEE J. Sel. Topics Appl. Earth Observ. Remote Sens.*, vol. 14, pp. 3811–3823, 2021.
- [79] J. Li et al., "Thin cloud removal fusing full spectral and spatial features for sentinel-2 imagery," *IEEE J. Sel. Topics Appl. Earth Observ. Remote Sens.*, vol. 15, pp. 8759–8775, 2022.
- [80] B. Zhao, J. Zhou, H. Xu, X. Feng, and Y. Sun, "PM-LSMN: A physical-model-based lightweight self-attention multiscale net for thin cloud removal," *IEEE Geosci. Remote Sens. Lett.*, vol. 21, 2024, Art. no. 5003405.
- [81] J. Gao, Q. Yuan, J. Li, H. Zhang, and X. Su, "Cloud removal with fusion of high resolution optical and SAR images using generative adversarial networks," *Remote Sens.*, vol. 12, no. 1, 2020, Art. no. 191.
- [82] H. Li, C. Gu, D. Wu, G. Cheng, L. Guo, and H. Liu, "Multiscale generative adversarial network based on wavelet feature learning for SAR-to-optical image translation," *IEEE Trans. Geosci. Remote Sens.*, vol. 60, 2022, Art. no. 5236115.
- [83] Y. Hao, W. Jiang, W. Liu, Y. Li, and B.-D. Liu, "Selecting information fusion generative adversarial network for remote-sensing image cloud removal," *IEEE Geosci. Remote Sens. Lett.*, vol. 20, 2023, Art. no. 6007605.

- [84] C. Li, X. Liu, and S. Li, "Transformer meets GAN: Cloud-free multispectral image reconstruction via multisensor data fusion in satellite images," *IEEE Trans. Geosci. Remote Sens.*, vol. 61, 2023, Art. no. 5408513.
- [85] P. Wang et al., "MTGAN: A SAR-to-optical image translation method for cloud removal," *ISPRS J. Photogrammetry Remote Sens.*, vol. 225, pp. 180–195, 2025.
- [86] F. Xu et al., "GLF-CR: SAR-enhanced cloud removal with global-local fusion," ISPRS J. Photogrammetry Remote Sens., vol. 192, pp. 268–278, 2022
- [87] Z. Wen, J. Suo, J. Su, B. Li, and Y. Zhou, "Edge-SAR-assisted multimodal fusion for enhanced cloud removal," *IEEE Geosci. Remote Sens. Lett.*, vol. 20, 2023, Art. no. 4009505.
- [88] C. Duan, M. Belgiu, and A. Stein, "Efficient cloud removal network for satellite images using SAR-optical image fusion," *IEEE Geosci. Remote Sens. Lett.*, vol. 21, 2024, Art. no. 6008605.
- [89] Y. Xia, W. He, Q. Huang, G. Yin, W. Liu, and H. Zhang, "CRformer: Multi-modal data fusion to reconstruct cloud-free optical imagery," *Int. J. Appl. Earth Observ. Geoinf.*, vol. 128, 2024, Art. no. 103793.
- [90] X. Zou et al., "DifCR: A fast conditional diffusion framework for cloud removal from optical satellite images," *IEEE Trans. Geosci. Remote Sens.*, vol. 62, 2024, Art. no. 5612014.
- [91] Y.-S. Shiu, M.-L. Lin, and T.-H. Chu, "Mapping and recovering cloud-contaminated area in multispectral satellite imagery with visible and near-infrared bands," in *Proc. IEEE Int. Geosci. Remote Sens. Symp.*, 2011, pp. 543–546.
- [92] Y. Shen, Y. Wang, H. Lv, and J. Qian, "Removal of thin clouds in landsat-8 OLI data with independent component analysis," *Remote Sens.*, vol. 7, no. 9, pp. 11481–11500, 2015.
- [93] M. Xu, M. Pickering, A. J. Plaza, and X. Jia, "Thin cloud removal based on signal transmission principles and spectral mixture analysis," *IEEE Trans. Geosci. Remote Sens.*, vol. 54, no. 3, pp. 1659–1669, Mar. 2016.
- [94] D. Tedlek, S. Khoomboon, T. Kasetkasem, T. Chanwimaluang, and I. Kumazawa, "A cloud-contamination removal algorithm by combining image segmentation and level-set-based approaches for remote sensing images," in Proc. Int. Conf. Embedded Syst. Intell. Technol. Int. Conf. Inf. Commun. Technol. Embedded Syst. (ICESIT-ICICTES), 2018, pp. 1–5.
- [95] M. Nagare, E. Kaneko, M. Toda, H. Aoki, and M. Tsukada, "Cloud shadow removal based on cloud transmittance estimation," in *Proc. IEEE Int. Geosci. Remote Sens. Symp.*, 2018, pp. 4031–4034.
- [96] M. Bertoluzza, C. Paris, and L. Bruzzone, "A fast method for cloud removal and image restoration on time series of multispectral images," in *Proc. 10th Int. Workshop Anal. Multitemporal Remote Sens. Images* (MultiTemp), IEEE, 2019, pp. 1–4.
- [97] H. Shen, J. Wu, Q. Cheng, M. Aihemaiti, C. Zhang, and Z. Li, "A spatiotemporal fusion based cloud removal method for remote sensing images with land cover changes," *IEEE J. Sel. Topics Appl. Earth Observ. Remote Sens.*, vol. 12, no. 3, pp. 862–874, Mar. 2019.
- [98] Q. Zhang, X. Liu, M. Liu, X. Zou, L. Zhu, and X. Ruan, "Comparative analysis of edge information and polarization on SAR-to-optical translation based on conditional generative adversarial networks," *Remote Sens.*, vol. 13, no. 1, 2021, Art. no. 128.
- [99] M. Zhang et al., "SAR-to-optical image translation via an interpretable network," *Remote Sens.*, vol. 16, no. 2, 2024, Art. no. 242.
- [100] Y. Huang, X. Ma, X. Zhang, and M.-O. Pun, "CycleGAN-based cloud removal from a feature enhancement perspective by transformer," in *Proc. IEEE Int. Geosci. Remote Sens. Symp.*, 2023, pp. 3772–3775.
- [101] S. Chen, X. Chen, J. Chen, and X. Cao, "A novel cloud removal method based on IHOT," in *Proc. IEEE Int. Geosci. Remote Sens. Symp.* (IGARSS), IEEE, 2016, pp. 449–452.
- [102] X. Ma, Y. Huang, X. Zhang, M.-O. Pun, and B. Huang, "Cloud-EGAN: Rethinking CycleGAN from a feature enhancement perspective for cloud removal by combining CNN and transformer," *IEEE J. Sel. Topics Appl. Earth Observ. Remote Sens.*, vol. 16, pp. 4999–5012, 2023.
- [103] J. Gao, H. Zhang, and Q. Yuan, "Cloud removal with fusion of SAR and optical images by deep learning," in *Proc. 10th Int. Workshop Anal. Multitemporal Remote Sens. Images (MultiTemp)*, IEEE, 2019, pp. 1–3.
- [104] Y. Li, R. Fu, X. Meng, W. Jin, and F. Shao, "A SAR-to-optical image translation method based on conditional generation adversarial network (CGAN)," *IEEE Access*, vol. 8, pp. 60338–60343, 2020.
- [105] S. Ghildiyal et al., "SSGAN: Cloud removal in satellite images using spatiospectral generative adversarial network," Eur. J. Agronomy, vol. 161, 2024, Art. no. 127333.

- [106] J. Zhang, J. Zhou, and X. Lu, "Feature-guided SAR-to-optical image translation," *IEEE Access*, vol. 8, pp. 70925–70937, 2020.
- [107] S. C. Kulkarni and P. P. Rege, "Pixel level fusion techniques for SAR and optical images: A review," *Inf. Fusion*, vol. 59, pp. 13–29, 2020.
- [108] Z. Zou, L. Chen, and X. Jiang, "Spectral-temporal low-rank regularization with deep prior for thick cloud removal," *IEEE Trans. Geosci. Remote Sens.*, vol. 62, 2023, Art. no. 5400916.
- [109] G. Zhou, C. Tian, C. Niu, G. Jing, H. Miao, and Z. Li, "Short time cloud-free image reconstruction based on time series images," *IEEE J. Sel. Topics Appl. Earth Observ. Remote Sens.*, vol. 16, pp. 51–65, 2023.
- [110] J. Lin, T.-Z. Huang, X.-L. Zhao, Y. Chen, Q. Zhang, and Q. Yuan, "Robust thick cloud removal for multitemporal remote sensing images using coupled tensor factorization," *IEEE Trans. Geosci. Remote Sens.*, vol. 60, 2022, Art. no. 5406916.
- [111] M. Xia and K. Jia, "Reconstructing missing information of remote sensing data contaminated by large and thick clouds based on an improved multitemporal dictionary learning method," *IEEE Trans. Geosci. Remote.* Sens., vol. 60, 2022, Art. no. 5605914.
- [112] W.-J. Zheng, X.-L. Zhao, Y.-B. Zheng, J. Lin, L. Zhuang, and T.-Z. Huang, "Spatial-spectral-temporal connective tensor network decomposition for thick cloud removal," *ISPRS J. Photogrammetry Remote Sens.*, vol. 199, pp. 182–194, 2023.
- [113] L.-Y. Li et al., "Thick cloud removal for multitemporal remote sensing images: When tensor ring decomposition meets gradient domain fidelity," *IEEE Trans. Geosci. Remote Sens.*, vol. 61, 2023, Art. no. 5512414.
- [114] S. Ji, P. Dai, M. Lu, and Y. Zhang, "Simultaneous cloud detection and removal from bitemporal remote sensing images using cascade convolutional neural networks," *IEEE Trans. Geosci. Remote Sens.*, vol. 59, no. 1, pp. 732–748, Jan. 2021.
- [115] Q. Zhang, Q. Yuan, J. Li, Z. Li, H. Shen, and L. Zhang, "Thick cloud and cloud shadow removal in multitemporal imagery using progressively spatio-temporal patch group deep learning," *ISPRS J. Photogrammetry Remote Sens.*, vol. 162, pp. 148–160, 2020.
- [116] C. Long, J. Yang, X. Guan, and X. Li, "Thick cloud removal from remote sensing images using double shift networks," in *Proc. 2021 IEEE Int. Geosci. Remote Sens. Symp.*, IEEE, 2021, pp. 2687–2690.
- [117] C. Stucker, V. S. F. Garnot, and K. Schindler, "U-TILISE: A sequence-to-sequence model for cloud removal in optical satellite time series," *IEEE Trans. Geosci. Remote Sens.*, vol. 61, 2023, Art. no. 5408716.
- [118] J. Lin, T.-Z. Huang, X.-L. Zhao, M. Ding, Y. Chen, and T.-X. Jiang, "A blind cloud/shadow removal strategy for multi-temporal remote sensing images," in *Proc. 2021 IEEE Int. Geosci. Remote Sens. Symp.*, IEEE, 2021, pp. 4656–4659.
- [119] T.-Y. Ji, D. Chu, X.-L. Zhao, and D. Hong, "A unified framework of cloud detection and removal based on low-rank and group sparse regularizations for multitemporal multispectral images," *IEEE Trans. Geosci. Remote* Sens., vol. 60, 2022, Art. no. 5303015.
- [120] Z. Tu, L. Guo, H. Pan, J. Lu, C. Xu, and Y. Zou, "Multitemporal image cloud removal using group sparsity and nonconvex low-rank approximation," *J. Nonlinear Variational Anal.*, vol. 7, no. 4, pp. 527–548, 2023
- [121] Q. Jiang, X.-L. Zhao, J. Lin, J.-H. Yang, J. Peng, and T.-X. Jiang, "Superpixel-oriented thick cloud removal method for multi-temporal remote sensing images," *IEEE Geosci. Remote Sens. Lett.*, vol. 21, 2023, Art. no. 5500805.
- [122] J.-L. Wang, X.-L. Zhao, H.-C. Li, K.-X. Cao, J. Miao, and T.-Z. Huang, "Unsupervised domain factorization network for thick cloud removal of multi-temporal remotely sensed images," *IEEE Trans. Geosci. Remote Sens.*, vol. 61, 2023, Art. no. 5405912.
- [123] Y. Chen, M. Chen, W. He, J. Zeng, M. Huang, and Y.-B. Zheng, "Thick cloud removal in multitemporal remote sensing images via low-rank regularized self-supervised network," *IEEE Trans. Geosci. Remote Sens.*, vol. 62, 2024, Art. no. 5506613.
- [124] B. Jiang et al., "A deep-learning reconstruction method for remote sensing images with large thick cloud cover," *Int. J. Appl. Earth Observ. Geoinf.*, vol. 115, 2022, Art. no. 103079.
- [125] P. Ebel, V. S. F. Garnot, M. Schmitt, J. D. Wegner, and X. X. Zhu, "UnCRtainTS: Uncertainty quantification for cloud removal in optical satellite time series," in *Proc. IEEE/CVF Conf. Comput. Vis. Pattern Recognit.*, 2023, pp. 2086–2096.
- [126] Y. Hao, W. Jiang, W. Liu, Y. Li, and B.-D. Liu, "Selecting information fusion generative adversarial network for remote sensing image cloud removal," *IEEE Geosci. Remote Sens. Lett.*, vol. 20, 2023, Art. no. 6007605.

- [127] Y. Zi, X. Song, F. Xie, and Z. Jiang, "Thick cloud removal in multitemporal remote sensing images using a coarse-to-fine framework," *IEEE Geosci. Remote Sens. Lett.*, vol. 21, 2024, Art. no. 6005605.
- [128] H. Zhou, Y. Wang, W. Liu, D. Tao, W. Ma, and B. Liu, "MSC-GAN: A multistream complementary generative adversarial network with grouping learning for multitemporal cloud removal," *IEEE Trans. Geosci. Remote Sens.*, vol. 63, 2025, Art. no. 5400117.
- [129] A. Sebastianelli et al., "PLFM: Pixel-level merging of intermediate feature maps by disentangling and fusing spatial and temporal data for cloud removal," *IEEE Trans. Geosci. Remote Sens.*, vol. 60, 2022, Art. no. 5412216.
- [130] Z. Wang, Q. Liu, X. Meng, and W. Jin, "Multi-discriminator supervision-based dual-stream interactive network for high-fidelity cloud removal on multitemporal SAR and optical images," *IEEE Geosci. Remote Sens. Lett.*, vol. 20, 2023, Art. no. 6012205.
- [131] H. Li, L. Zhang, and H. Shen, "A principal component based haze masking method for visible images," *IEEE Geosci. Remote Sens. Lett.*, vol. 11, no. 5, pp. 975–979, May 2014.
- [132] C.-H. Lin, P.-H. Tsai, K.-H. Lai, and J.-Y. Chen, "Cloud removal from multitemporal satellite images using information cloning," *IEEE Trans. Geosci. Remote Sens.*, vol. 51, no. 1, pp. 232–241, Jan. 2013.
- [133] Q. Cheng, H. Shen, L. Zhang, Q. Yuan, and C. Zeng, "Cloud removal for remotely sensed images by similar pixel replacement guided with a spatio-temporal MRF model," *ISPRS J. Photogrammetry Remote Sens.*, vol. 92, pp. 54–68, 2014.
- [134] X. Li, H. Shen, L. Zhang, H. Zhang, Q. Yuan, and G. Yang, "Recovering quantitative remote sensing products contaminated by thick clouds and shadows using multitemporal dictionary learning," *IEEE Trans. Geosci. Remote Sens.*, vol. 52, no. 11, pp. 7086–7098, Nov. 2014.
- [135] B. Chen, B. Huang, L. Chen, and B. Xu, "Spatially and temporally weighted regression: A novel method to produce continuous cloud-free landsat imagery," *IEEE Trans. Geosci. Remote Sens.*, vol. 55, no. 1, pp. 27–37, Jan. 2017.
- [136] X. Li, H. Shen, H. Li, and L. Zhang, "Patch matching-based multitemporal group sparse representation for the missing information reconstruction of remote-sensing images," *IEEE J. Sel. Topics Appl. Earth Observ. Remote Sens.*, vol. 9, no. 8, pp. 3629–3641, Aug. 2016.
- [137] Q. Zhang, Q. Yuan, Z. Li, F. Sun, and L. Zhang, "Combined deep prior with low-rank tensor SVD for thick cloud removal in multitemporal images," *ISPRS J. Photogrammetry Remote Sens.*, vol. 177, pp. 161–173, 2021.
- [138] Q. Zhang, F. Sun, Q. Yuan, and L. Zhang, "Thick cloud removal for sentinel-2 time-series images via combining deep prior and low-rank tensor completion," in *Proc. 2021 IEEE Int. Geosci. Remote Sens. Symp.*, IEEE, 2021, pp. 2675–2678.
- [139] S. Imran, M. Tahir, Z. Khalid, and M. Uppal, "A deep unfolded prioraided RPCA network for cloud removal," *IEEE Signal Process. Lett.*, vol. 29, pp. 2048–2052, 2022.
- [140] Q. Zhang, Q. Yuan, C. Zeng, X. Li, and Y. Wei, "Missing data reconstruction in remote sensing image with a unified spatial-temporal-spectral deep convolutional neural network," *IEEE Trans. Geosci. Remote Sens.*, vol. 56, no. 8, pp. 4274–4288, Aug. 2018.
- [141] Y. Chen, L. Tang, X. Yang, R. Fan, M. Bilal, and Q. Li, "Thick clouds removal from multitemporal ZY-3 satellite images using deep learning," *IEEE J. Sel. Topics Appl. Earth Observ. Remote Sens.*, vol. 13, pp. 143–153, 2019.
- [142] Y. Chen, Q. Weng, L. Tang, X. Zhang, M. Bilal, and Q. Li, "Thick clouds removing from multitemporal landsat images using spatiotemporal neural networks," *IEEE Trans. Geosci. Remote Sens.*, vol. 60, 2020, Art. no. 4400214.
- [143] M. Xu, X. Jia, M. Pickering, and A. J. Plaza, "Cloud removal based on sparse representation via multitemporal dictionary learning," *IEEE Trans. Geosci. Remote Sens.*, vol. 54, no. 5, pp. 2998–3006, May 2016.
- [144] X. Li, L. Wang, Q. Cheng, P. Wu, W. Gan, and L. Fang, "Cloud removal in remote sensing images using nonnegative matrix factorization and error correction," *ISPRS J. Photogrammetry Remote Sens.*, vol. 148, pp. 103–113, 2019.
- [145] P. Ebel, Y. Xu, M. Schmitt, and X. X. Zhu, "SEN12MS-CR-TS: A remotesensing data set for multimodal multitemporal cloud removal," *IEEE Trans. Geosci. Remote Sens.*, vol. 60, 2022, Art. no. 5222414.
- [146] Y. Xia, H. Zhang, L. Zhang, and Z. Fan, "Cloud removal of optical remote sensing imagery with multitemporal SAR-optical data using X-Mtgan," in *Proc. IEEE Int. Geosci. Remote Sens. Symp.*, IEEE, 2019, pp. 3396–3399.

- [147] J. D. Bermudez, P. N. Happ, R. Q. Feitosa, and D. A. Oliveira, "Synthesis of multispectral optical images from SAR/optical multitemporal data using conditional generative adversarial networks," *IEEE Geosci. Remote Sens. Lett.*, vol. 16, no. 8, pp. 1220–1224, Aug. 2019.
- [148] R. Mao, H. Li, G. Ren, and Z. Yin, "Cloud removal based on SAR-optical remote sensing data fusion via a two-flow network," *IEEE J. Sel. Topics Appl. Earth Observ. Remote Sens.*, vol. 15, pp. 7677–7686, 2022.
- [149] D. Lin, G. Xu, X. Wang, Y. Wang, X. Sun, and K. Fu, "A remote sensing image dataset for cloud removal," 2019, arXiv:1901.00600.
- [150] P. Ebel, A. Meraner, M. Schmitt, and X. X. Zhu, "Multisensor data fusion for cloud removal in global and all-season sentinel-2 imagery," *IEEE Trans. Geosci. Remote Sens.*, vol. 59, no. 7, pp. 5866–5878, Jul. 2021.
- [151] M. Wang, Y. Song, P. Wei, X. Xian, Y. Shi, and L. Lin, "IDF-CR: Iterative diffusion process for divide-and-conquer cloud removal in remote-sensing images," *IEEE Trans. Geosci. Remote Sens.*, vol. 62, 2024, Art. no. 5615014.
- [152] X. Qin, Z. Wang, Y. Bai, X. Xie, and H. Jia, "FFA-Net: Feature fusion attention network for single image dehazing," in *Proc. AAAI Conf. Artif. Intell.*, 2020, pp. 11908–11915.
- [153] K. Chi, Y. Yuan, and Q. Wang, "Trinity-net: Gradient-guided swin transformer-based remote sensing image dehazing and beyond," *IEEE Trans. Geosci. Remote Sens.*, vol. 61, 2023, Art. no. 4702914.
- [154] H. Sun et al., "Partial siamese with multiscale bi-codec networks for remote sensing image haze removal," *IEEE Trans. Geosci. Remote Sens.*, vol. 61, 2023, Art. no. 4106516.
- [155] L. Zhang and S. Wang, "Dense haze removal based on dynamic collaborative inference learning for remote sensing images," *IEEE Trans. Geosci. Remote Sens.*, vol. 60, 2022, Art. no. 5631016.
- [156] Y. Song, Z. He, H. Qian, and X. Du, "Vision transformers for single image dehazing," *Trans. Img. Process.*, vol. 32, pp. 1927–1941, 2023.
- [157] Y. Wen, T. Gao, J. Zhang, Z. Li, and T. Chen, "Encoder-free multi-axis physics-aware fusion network for remote sensing image dehazing," *IEEE Trans. Geosci. Remote Sens.*, vol. 61, 2023, Art. no. 4705915.
- [158] Y. Cui, W. Ren, X. Cao, and A. Knoll, "Revitalizing convolutional network for image restoration," *IEEE Trans. Pattern Anal. Mach. Intell.*, vol. 46, no. 12, pp. 9423–9438, Dec. 2024.
- [159] Y. Cui and A. Knoll, "Exploring the potential of channel interactions for image restoration," *Knowl.-Based Syst.*, vol. 282, 2023, Art. no. 111156.
- [160] A. Meraner, P. Ebel, X. X. Zhu, and M. Schmitt, "Cloud removal in sentinel-2 imagery using a deep residual neural network and SARoptical data fusion," *ISPRS J. Photogrammetry Remote Sens.*, vol. 166, pp. 333–346, 2020.
- [161] V. S. Fare Garnot and L. Landrieu, "Panoptic segmentation of satellite image time series with convolutional temporal attention networks," in *Proc. IEEE/CVF Int. Conf. Comput. Vis.*, 2021, pp. 4852–4861.



Jin Ning received the B.S. degree in computer science and technology and the Ph.D. degree in computer science and technology from the University of Electronic Science and Technology, Chengdu, China, in 2014 and 2020, respectively.

She is currently a Lecturer with Chengdu University of Technology. Her current research interests include computer vision, remote sensing, and data mining.



Lianbin Xie received the B.S. degree in computer science and technology from Chengdu Normal University, Chengdu, China, in 2023. He is currently working toward the M.S. degree in computer science and technology with the Chengdu University of Technology, Chengdu.

His research interests include computer vision and cloud removal.



Jie Yin received the B.S. degree in software engineering from the Chengdu University of Information Technology, Chengdu, China, in 2023. She is currently working toward the M.S. degree in computer science and technology with Chengdu University of Technology, Chengdu, China.

Her research interests include computer vision and image dehazing.



Yiguang Liu received the B.S. degree in mechanical engineering from the Nanjing University of Science and Technology, Nanjing, China, in 1995, the M.S. degree in mechanics from Peking University, Beijing, China, in 1998, and the Ph.D. degree in computer science and technology from Sichuan University, Chengdu, China, in 2004.

He has been a Research Fellow with the National University of Singapore, Singapore, a Visiting Professor with Imperial College London, London, U.K., and a Senior Research Scholar with Michigan State

University, East Lansing, MI, USA. He is currently the Haina Distinguished Professor with the College of Computer Science, Sichuan University. He has authored or coauthored more than 100 articles published in IEEE TRANSACTIONS ON GEOSCIENCE AND REMOTE SENSING, IEEE TRANSACTIONS ON IMAGE PROCESSING, IEEE TRANSACTIONS ON NEURAL NETWORKS AND LEARNING SYSTEMS, ICCV, CVPR, OSA OL, OE, and AIP APL. His research interests include information probe and the related intelligent perception.

Dr. Liu was the recipient of several paper awards such as IEEE ICME BSTA in 2017.